Responsive glazing systems: Characterisation methods, summer performance and implications on thermal comfort

Nomenclature

E	specific energy (Wh/m^2)
g	solar factor (-)
H	specific incident daily solar radiation (kWh/m^2)
HF	Heat Flux (W/m^2)
I	specific incident solar irradiance (W/m^2)
$\dot{q}$	specific heat flux (W/m^2)
t	time (h)
U	thermal transmittance (W/m^{2}K)

Greek symbols

τ	transmission coefficient (-)
ϑ	temperature (°C)

Superscripts

*	referred to an equivalent value or a modified index

Subscripts

air	referred to air
average	referred to an average value
bn	beam normal
day	referred to day between sunrise and sunset
$\Delta\theta$	referred to temperature difference
e	solar
ex	excursion
i	referred to heat flux released to the indoor environment
in	referred to the indoor environment
n	referred to normalised energy
out	referred to the outdoor environment
sol	referred to solar energy
surf	referred to the surface
tot	total including long-wave and short-wave radiation
v	visible
24	referred to daily energy

Acronyms

CDD	Cooling Degree Days
ERF	Effective radiant field (W/m^2)
PMV	Predicted Mean Vote (-)
PPD	Predicted Percentage of Dissatisfied (%)
RMSE	Root Mean Square Error
TT	Thermotropic glazing
TGU	Triple Glazing Unit, reference technology
TGU_TT	Triple Glazing Unit with thermotropic glazing
TGU_TT+PCM(IN)	Triple Glazing Unit with thermotropic glazing and a PCM-filled cavity in the inner position
TGU_TT+PCM(OUT)	Triple Glazing Unit with thermotropic glazing and a PCM-filled cavity in the outer position

Highlights:

- Two responsive windows with PCM and thermotropic panes were tested in a test cell
- Daily and long-term performance analyses were carried out under summer conditions
- The energy performance and thermal comfort of the glazing were assessed
- PCM in the cavity of a triple glazing unit improves thermal comfort
- Integrating a thermotropic pane in a triple glazing unit may reduce cooling loads

Abstract:

In recent years, there have been several experimental and numerical researches on transparent envelope components that integrate phase change materials (PCMs). To address some of the drawbacks of these systems, new prototypes were created and their summer performance was monitored under Cfa climatic conditions (Turin, Italy). The proposed glazing system comprises a triple glazing unit with a thermotropic layer placed on the outer side, acting as a switchable shading system capable of regulating the phase transition of the PCM. The PCM is tested in both the inner and the outer cavity of the glazing, alternately. In this paper, the summer performance of these responsive glazing systems is reported, complementing the assessment of their performance under winter conditions, which was previously presented in another paper (Bianco et al., 2017). Two additional systems were also tested in parallel for reference purposes: a triple glazing unit with a thermotropic layer only, and a reference triple glazing unit. Direct solar transmission was assessed, and the correlation between glazing temperature and solar transmission coefficient of the thermotropic layer, when coupled with the triple glazing unit, was derived. The solar transmission as a function of the external surface temperature of the PCM glazing units was also evaluated. The energy performance was assessed by means of a long-term evaluation in addition to daily analyses during cloudy and sunny days. The capability of the aforementioned technologies to improve indoor thermal comfort was investigated, with the effect of the transmitted solar radiation impinging on the occupants also taken into account. The results highlight that the integration of a thermotropic layer in a triple glazing unit allows the cooling load through the transparent component to be reduced by one third when compared to a traditional triple glazing unit. The overall energy performance was found to be primarily affected by the position of the PCM; not only during winter season, but especially in summer, the PCM completed the phase transition only when placed in the outermost cavity. The thermal comfort conditions were improved, when evaluated in terms of traditional PMV, regardless of the position of the PCM layer. However, when the influence of the direct solar radiation impinging on the occupants was taken into account, the solution with the PCM layer located in the inner cavity presented a better performance.

Keywords: window systems, responsive glazing, dynamic component, PCM, thermotropic glass, switchable glazing, solar factor, g value, energy performance, thermal comfort, PMV.

1. Introduction

Transparent envelope components are key elements in buildings. They affect building energy performance and daylighting, and therefore have a significant effect on both thermal and visual comfort. To improve these aspects throughout the year, an accurate seasonal control of solar gains, heat losses and light gains is desirable. Dynamic glazing systems capable of modifying their thermo-optical properties according to defined boundary conditions are promising solutions to address this need (Favoino et al., 2015).

Dynamic behaviour in glazing systems can be achieved by several means. Thermochromic and thermotropic materials have been developed – characterised by the temperature dependency of their solar/visible absorption coefficient and their transmission mode (direct-to-direct or diffuse transmission), respectively (Seeboth et al., 2010). In this way, these systems can modulate the transmitted solar radiation, rejecting most of it during hot summer days, yet allowing a certain amount of solar gain to enter the building during cold winter days (Allen et al., 2017; Yao and Zhu, 2012).

Another way to achieve dynamic behaviour of glazing systems is by introducing a phase change material (PCM) within the gap of a double (Goia et al., 2014b; Gowreesunker et al., 2013) or triple glazing unit (S. Li et al., 2016), or within more-complex glazing components (Grynning et al., 2015, 2013). PCMs in glazing systems notably increase their inertial behaviour, smoothing the indoor surface temperature and providing peak load shifting. The PCM interacts with the incident solar radiation, acting both as a solar shading device and a heat storage medium. When in solid state, the PCM blocks most of the incident solar radiation, which is absorbed, causing the PCM to undergo phase change and eventually melt. During this process, a great amount of heat is stored by the PCM, preventing it from turning into a cooling load during the summer season. Furthermore, during the phase transition, the optical properties of the PCM are subject to a change: the transmission coefficient increases. This allows a much greater amount of solar radiation to enter the indoor environment when the PCM is fully melted. During the night, the PCM solidifies and releases the stored heat. According to the glazing configuration, this heat can be released mostly towards either the external or internal environment.

The performance of PCM-enhanced glazing components was investigated by several experimental (Goia et al., 2014b, 2013; Gowreesunker et al., 2013; S. Li et al., 2016) and numerical (Goia, 2012; Ismail et al., 2008; Zhong et al., 2015) studies. A review of PCM technologies developed for transparent and translucent building envelope components can be found in (Silva et al., 2016).

Ad-hoc numerical models were specifically developed to take the interaction of PCM with solar radiation into account (Goia et al., 2012a; Ismail and Henríquez, 2002; Liu et al., 2016). With regard to the transparent components, not only

the thermophysical but also the optical properties of PCMs play an important role in the thermal performance of PCM-filled glazing units (D. Li et al., 2016a, 2016b). Therefore, solar and visible properties are needed for a complete and accurate analysis of the behaviour of such components (Goia et al., 2015, 2012b; Li et al., 2015) and for a comprehensive evaluation, both thermal and visual aspects should be considered (Giovannini et al., 2017).

Other than contributing to improvements in the energy performance of buildings, the inclusion of PCM in glazing systems can have a positive effect on thermal comfort (Goia et al., 2013). However, the melting temperature of the PCM needs to be carefully selected according to the climate. During summer in particular, if complete melting of the PCM within a double glazing unit occurs before sunset, then the internal surface temperature of the glazing may increase to a level that may negatively affect thermal comfort (Goia et al., 2013).

Even though PCM-filled double glazing units have been proven to be beneficial in several ways, the introduction of PCM in a double glazing unit results in a reduced thermal resistance, negatively affecting the thermal performance of the system. In addition, seasonal control of the direction of the heat flux released during the night-time discharging phase (mostly towards the indoor or outdoor environment) would be desirable (Goia et al., 2014b). To address this, a novel technology that combines a PCM-filled triple glazing unit with a thermotropic layer was proposed (Bianco et al., 2017; Goia et al., 2014a). The use of a thermotropic layer can offer better control of the charging phase of the PCM. In addition, combining a PCM with a gas-filled gap in a triple glazing unit improves the thermal resistance of the system and can also offer better control of the discharging phase according to the position of the PCM.

For the tests conducted on this newly proposed technology, PCM (paraffin wax with a melting range between 33 °C and 37 °C and peak melting temperature of 35 °C) was used in the inner or the outer cavity of the triple glazing, alternately, while the second cavity was filled with 90% Argon and presented a low-e coating. In this way, only a slight decrease of the thermal resistance of the glazing was achieved (compared to a conventional triple glazing unit). The melting temperature of the PCM was selected in accordance with a previous experimental study carried out in Turin, where it was demonstrated to be suitable for the local climate. The thermotropic layer, which was a commercially available product, was always placed as the outermost layer. The behaviour of the thermotropic layer alone, when coupled with a triple glazing unit without the inclusion of PCM, was also monitored. Overall, the following technologies were tested (refer to Appendix 1):

- A reference low-e triple glazing unit with 90% Argon (TGU);
- The TGU with an adjacent thermotropic layer on the outer side (TGU_TT);

- The TGU with its inner cavity filled with PCM and an adjacent thermotropic layer on the outer side (TGU_TT+PCM(IN)); and
- The TGU with its outer cavity filled with PCM and an adjacent thermotropic layer on the outer side (TGU_TT+PCM(OUT)).

The cost of the triple glazing unit was estimated to be 30% higher than a simple double glazing unit, whereas the cost of the TGU_TT and TGU_TT+PCM prototypes were about 2.1 and 2.6 times that of the reference TGU, respectively. If they were to progress to industrial production, however, then costs can be expected to decrease.

A comprehensive description of this technology and a detailed analysis of its performance during the winter seasons is presented in Bianco et al., (2017). In syntheses, the following key issues emerged during this study:

- In clear sky conditions, the PCM in the outer cavity (TGU_TT+PCM(OUT)) showed an interesting dynamic range, which led to a significant improvement in the thermal behaviour of the system compared to the reference TGU; the overheating problem during the central hours of the day was mitigated, with the exploitation of the solar free gains shifted to the evening hours, when the heating energy demand is higher.
- The adoption of the PCM in the inner cavity of the glazing (TGU_TT+PCM(IN)) was not found to be beneficial in winter. Neither was the application of the thermotropic layer alone (TGU_TT). The results showed that, during cloudy winter days, the position of the PCM does not influence the overall performance of the prototype, since it never changed phase. On the other hand, during sunny winter days, the glazing with the PCM in the outer position did undergo phase transition and presented a slightly better performance than the TGU_TT+PCMC(IN).

Further data on the winter performance is reported in this paper in Section 4. Nevertheless, in order to properly and completely characterise the behaviour of a building component and to suitably judge its potential application in buildings, a whole year analysis is needed. For this reason, the present paper focuses on the analysis of the summer performance of these new technologies and on their effect on thermal comfort. Specifically, the following studies are presented in detail:

- Characterisation of the thermophysical properties (i.e. direct solar transmission and equivalent solar factor);
- Characterisation of the energy performance under summer conditions (both daily and long-term performance evaluations); and
- Thermal comfort analyses (in terms of predicted mean vote (PMV) and modified PMV indices).

2. Methods and Parameters

The complete description of materials, technologies and experimental test rig was presented in Bianco et al. (2017). For the sake of brevity, only a summary is presented here. The experimental campaign, which took place between March 2013 and April 2015, was carried out in the TWINS outdoor test facility, located on the rooftop of the Polytechnic University of Turin (Politecnico di Torino). The indoor temperature was set to 26 °C during the summer season. More than 30 sensors were positioned on the technologies, which were mounted on the south façade of the test cell. Data was recorded every five minutes. Surface and air temperatures were measured with TT-type thermocouples, that were pre-calibrated in the laboratory. Heat flux meters and pyranometers were used to measure the heat and solar fluxes for each glazing (see Figure 3 in Bianco et al. (2017) for the position of the sensors). The TGU, TGU_TT and TGU_TT+PCM technologies were tested simultaneously; however, the TGU_TT+PCM was alternately monitored with the PCM in the inner and outer cavity by rotating the prototype.

2.1 Types of analyses and representative boundary conditions

The analyses began with the assessment of equivalent solar factor and solar transmission coefficient of each technology under investigation. Then, the following two kinds of analyses, which were first adopted in Bianco et al. (2017), were used to assess the energy performance of the proposed technologies and the reference:

- Daily analyses during cloudy and sunny days; and
- A long-term energy performance evaluation over a period of 21 days (between June and September);

A set of 30 days (between June and September) was selected to evaluate the equivalent solar factor. The indoor thermal comfort of a hypothetical indoor environment enclosed with the investigated technologies was also assessed (more details are reported in Paragraph 3.2.5).

The daily analyses were conducted by selecting four different days, two with low solar irradiance (Day 5 and Day 6 – cloudy days) and two with high solar irradiance (Day 7 and Day 8 – sunny days), as reported in Table 1. The performance of the technologies with PCM placed in the inner and in the outer cavity and that of the TGU_TT during the selected days was compared against the reference TGU.

Table 1 – Boundary conditions of the selected days: solar irradiation, average external air temperature and external air temperature excursion.

		H	$\vartheta_{air,out,average}$	ϑ_{ex}
		$[kWh/m^2]$	$[°C]$	$[°C]$
TGU_TT+PCM(IN)	*Day 5 hot+cloudy*	*1.1*	*21.7*	*5.5*

TGU_TT+PCM(OUT)	*Day 6 hot+cloudy*	*1.4*	*19.3*	*5.4*
TGU_TT+PCM(IN)	*Day 7 hot+sunny*	*2.9*	*29.1*	*10.2*
TGU_TT+PCM(OUT)	*Day 8 hot+sunny*	*3.7*	*27.5*	*11.6*

Representative days were selected to evaluate the performance of the proposed technologies under comparable boundary conditions. To select appropriate days and assess their representativeness, a double frequency distribution analysis of the daily mean external temperature and the global vertical irradiation monitored for the whole duration of the experimental campaign was performed (Figure 1) (Bianco et al., 2017). This frequency analysis was plotted as a colour coded area: the darker the area on the graph, the higher the number of days characterised by the corresponding global vertical irradiation and daily mean external air temperature.

As shown in Figure 1a, the cloudy days (Day 5 and Day 6) selected for the daily analyses fall in an area simultaneously characterised by low global solar irradiation and low mean temperatures with respect to the temperature range measured during the summer season. In contrast, the sunny days (Day 7 and Day 8) were chosen among the extreme temperature values with similar global solar irradiation. The hourly boundary conditions of the days selected for the daily analyses are reported in Figure 2.

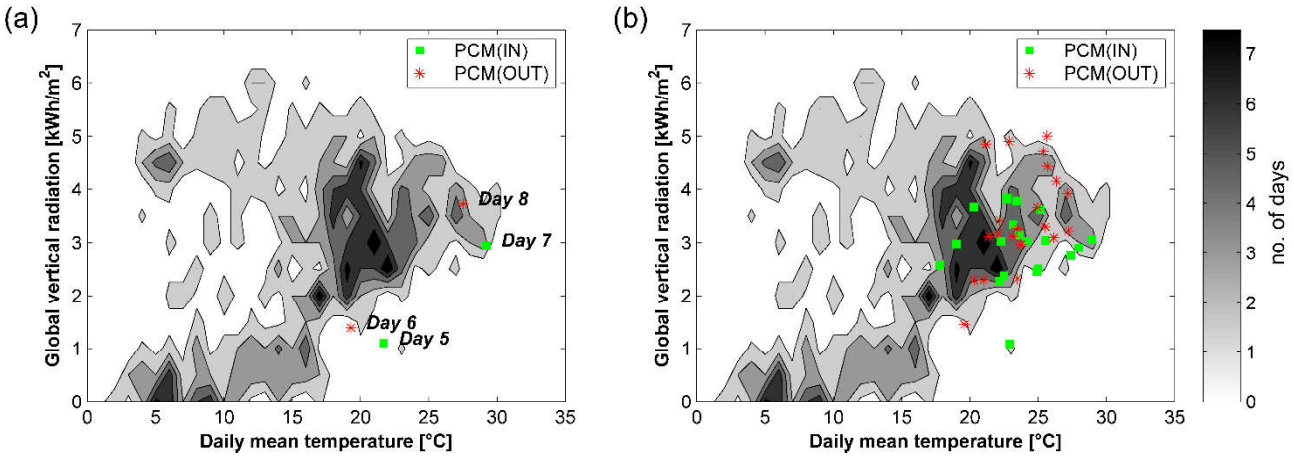

Figure 1 – Frequency distribution of the weather data expressed as the number of days having the same relationship of global vertical irradiation and daily mean temperature; (a) days selected for daily analysis, (b) days selected for the long-term performance evaluation.

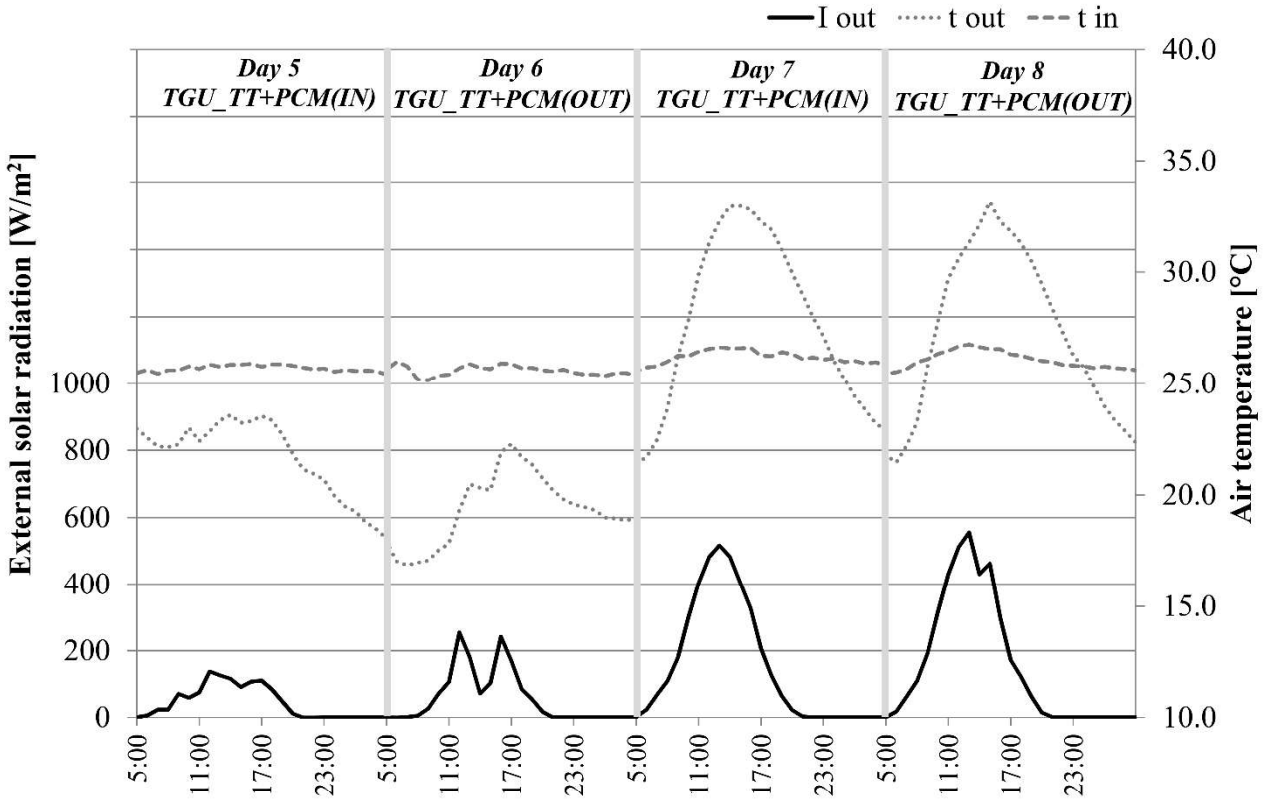

Figure 2 – Boundary conditions of the selected days; hourly time profiles of external solar radiation and air temperature.

2.2 Performance parameters

2.2.1 Direct solar transmission (τ_e)

For all the technologies, the direct solar transmission (τ_e) was assessed as the ratio of solar radiation measured by the internal vertical pyranometer and the solar radiation measured by the external vertical pyranometer (please refer to Paragraph 2.6.2, Equation 1, in Bianco et al., 2017).

The correlation between the solar transmission coefficient of the TGU_TT and glazing temperature was estimated through linear regression by assuming the solar transmission coefficient to be constant in the *on* and *off* states and to change linearly in between (Bianco et al., 2015). In this way, the regression had the form of a double-change-point problem. The regression coefficients were evaluated with the "Inverse Modeling Toolkit" (IMT) (Kissok et al., 2003) by decomposing the double-change-point problem into two separate three-parameter (3P) change-point problems (Kissok et al., 1994). A graphical description of the adopted regression correlations is provided in Figure 3 and their analytical formulations are described by Equation 1.

$$\begin{cases} \tau_e(\vartheta) = \tau_{e,off} + \beta_2 \cdot (\vartheta - \vartheta_{off})^+ & \text{if } \vartheta < \vartheta_{on} \\ \tau_e(\vartheta) = \tau_{e,on} + \beta_2 \cdot (\vartheta - \vartheta_{on})^- & \text{if } \vartheta > \vartheta_{off} \end{cases}$$

Equation 1

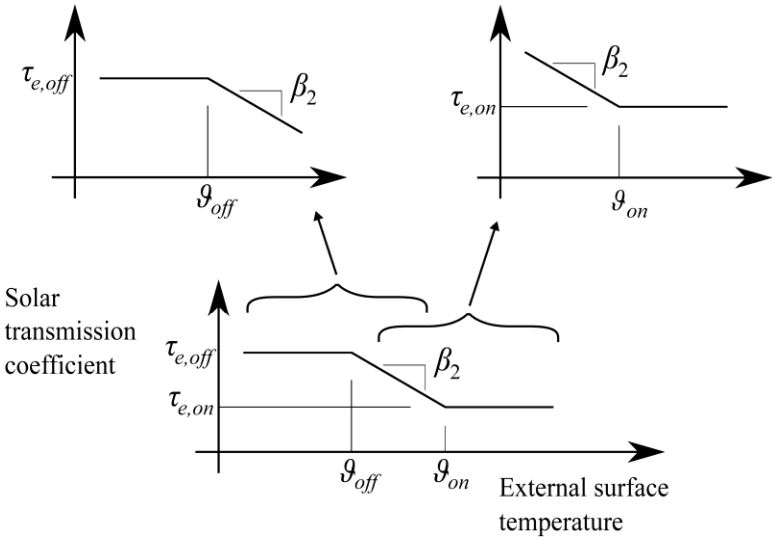

Figure 3 – Regression model for the evaluation of the solar transmission coefficient of the TGU_TT as a function of the external surface temperature.

For this purpose, the monitored dataset was divided into two portions to find the regression equations and several combinations of temperature values were tested to split the data. Among the pairs of fits having the same slope for the left and right sections of the plots, the pair that guaranteed the best overall fit, evaluated in terms of lowest root-mean-square error, was chosen.

Before evaluating the regression coefficients, a pre-processing of the data was performed. First, the outliers of the whole dataset were detected and removed. Second, the outliers among the values ranging within each degree of temperature were also filtered. Tukey's box plot outlier detection technique was adopted (Tukey, 1977).

The solar transmission as a function of the external surface temperature of the PCM glazing was also evaluated. The same days selected to analyse the normalised energy were used to evaluate the solar transmission. Only selected hours, between 10:00 and 14:00, were used. The trend of the solar transmission was assessed over 120 readings with hourly time step for both TGU_TT+PCM(IN) and TGU_TT+PCM(OUT) (see Paragraph 3.1.1, solar transmission coefficient).

2.2.2 Equivalent solar factor (g*-value)

The solar factor (*g-value*) is defined as the fraction of solar radiation that enters through a window, as the sum of the directly transmitted solar radiation and the secondary heat flux absorbed by the glazing and then released to the indoor environment by convection and longwave IR-radiation (ISO 9050, 2003), (see Figure 4).

During the experimental activity in the test cell exposed to real boundary conditions, the transmitted solar radiation could be directly measured by means of an internal pyranometer, and the solar transmission coefficient could be subsequently calculated (see Paragraph 2.2.1). Contrastingly, the second variable required in order to assess *g-value* – the heat flux absorbed by the glazing and released to the indoor environment – could not be directly measured in the field. A heat flux meter positioned on the inner skin of the glazing measures the totality of the surface heat flux exchanged between the glazing and the environment, which includes the contribution due to the temperature difference and that due to the heat flux absorbed by the glazing and released to the indoor environment. Since only a part of this second variable is needed in order to evaluate the solar factor, and since it cannot be separately measured, a simplified calculation methodology was applied to evaluate an equivalent solar factor (*g*-value*). This calculation allows the evaluation of an average daily result for *g*-value*. A daily parameter is not optimal for responsive glazing systems that modify their properties throughout the day, but the results still allow for discussion of the behaviour of the tested windows.

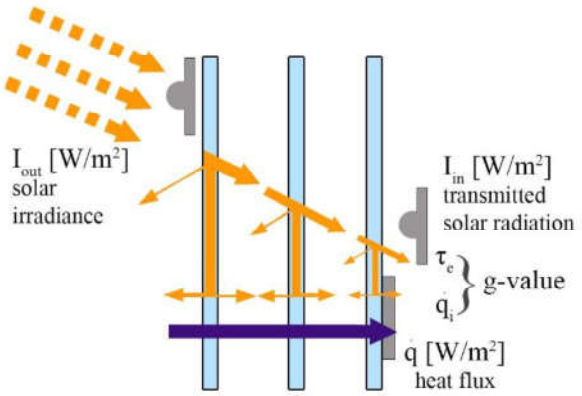

Figure 4 – Schematic view of the heat flux exchanged in a glazing component showing sensor positions.

The equivalent solar factor was evaluated according to Equation 2 (Bianco, 2014; Bianco et al., 2015) as the ratio of the difference between the daily total energy crossing the component ($E_{day,tot}$) and the energy exchanged due to temperature difference ($E_{day,\Delta\theta}$) on the daily solar energy incident on the façade ($E_{day,sol,out}$). In this way it was possible, on a daily basis, to remove the energy exchanged for the effect of the temperature difference between indoor and outdoor environment. Energies were calculated as the integral of the fluxes between sunrise and sunset. $E_{day,tot}$ was evaluated

according to Equation 2 in Bianco et al. (2017), but with a different time of integration, whereas $E_{day,\Delta\theta}$ was calculated as the product of the difference between internal and external air temperatures and the equivalent thermal transmittance evaluated as discussed in Bianco et al. (2017). The selected days were chosen from those used for the long-term analyses, with only those days with a daily solar energy incident on the south façade greater than 2000 Wh/m^2 being used for the evaluation of the g*-value. Half of the days belonged to the dataset with the PCM placed in the inner cavity, while the other half belonged to the dataset with the PCM placed in the outer cavity.

$$g^* = \frac{E_{day,tot} - E_{day,\Delta\theta}}{E_{day,sol,out}} = \frac{\int_{sunrise}^{sunset} \left(\dot{q}_{surf} + I_{in}\right) \mathrm{d}t - \int_{sunrise}^{sunset} U \cdot \left(\vartheta_{\mathrm{out}} - \vartheta_{in}\right) \mathrm{d}t}{\int_{sunrise}^{sunset} I_{out} \mathrm{d}t}$$

Equation 2

It should be noted that the equivalent solar factor can be expected to be lower than the traditional *g-value*, due to the different incidence angle and convective/radiative heat exchange that occurs in the field; for measurements performed in the lab according to a standardised procedure, the radiation incident on the sample is perpendicular to it, and the secondary transmission is equally divided between the indoor and the outdoor faces of the sample.

2.2.3 Daily energies

The same symbols and methodology applied for the heating season (Bianco et al., 2017) were used for the cooling season. Total daily energies ($E_{24,tot}$) were calculated as the integral over the day of the total heat flux (given by the sum of the indoor surface heat flux measured with the heat flux meters and of the transmitted solar irradiance measured with the pyranometer) according to Equation 3. The starting integration time was chosen at 05:00 to exclude the effect of the previous day on the analysis of the data.

$$E_{24,tot} = \int_{05:00}^{05:00+1day} \dot{q}_{tot} \, \mathrm{d}t$$

Equation 3

2.2.4 Long-term total energy

Two sets of 21 days were selected for the long-term performance evaluation. The first set considered the PCM positioned in the inner cavity (TGU_TT+PCM(IN)), whereas for the second set, the PCM was positioned in the outer cavity (TGU_TT+PCM(OUT)). The boundary conditions of each day are reported in Figure 1b. A wide variety of

combinations of external air temperature and solar radiation were taken into account for this analysis. To provide a reliable comparison between the two datasets, similar boundary conditions were selected in terms of cooling degree days (CDD). CDD values of 45.6 °C·Day and 45.9 °C·Day were calculated for the two periods, according to Equation 4, respectively, for TGU_TT+PCM(IN) and TGU_TT+PCM(OUT). The comparability of the two long-term periods was confirmed by analysing the total solar irradiation incident on the south façade of the test cell; the values found were 73.6 kWh/m^2 and 75.3 kWh/m^2 for TGU_TT+PCM(IN) and TGU_TT+PCM(OUT), respectively.

First, the daily maximum values of the total heat flux were compared between the three technologies during the selected days. Then, normalised total energies ($E_{n,tot}$) were evaluated over the two sets as the ratio of the total energy to the cooling degree days, according to Equation 5.

$$CDD = \sum_{day=1}^{n} (\overline{\vartheta}_{in} - \overline{\vartheta}_{out})$$

Equation 4

$$E_{n,tot} = \frac{\int_{05:00}^{05:00+1day} \dot{q}_{tot} \, \mathrm{d}t}{CDD}$$

Equation 5

2.2.5 Predicted mean vote (PMV) and modified PMV (PMV*)

In addition to the energy performance analyses, the capability of the tested technologies to improve the indoor global thermal comfort was investigated in accordance with the methodology reported in Goia et al. (2013). The predicted mean vote (PMV), as proposed by P. O. Fanger in 1970, was calculated according to the standard ISO 7730 (EN, 2005) by means of a software tool (HyperComfort) developed by Politecnico di Torino, Dept. of Energy (following the standard ISO 7730 (EN, 2005)). Spatial distributions of the PMV index were calculated assuming the following hypotheses:

- The size of the simulated room was 3 × 7 × 3 m;

- The south façade, where the tested technologies were mounted, was modelled as entirely glazed, and the transparent façade was considered to comprise only one type of prototype glazing, having a uniform surface temperature;
- The south façade was the only surface exposed to external boundary conditions. The measured internal surface temperature of the glazing and internal air temperature were inputs to the model. The surface temperatures of the ceiling, floor and the other walls were assumed to be the same as the internal air;
- The simulations were launched for the hours of peak conditions of Day 7 and Day 8, when the highest internal surface temperature on the glazing technologies was reached;
- Relative humidity and air velocity were assumed equal to their standard values, 50% and 0.1 m/s; and
- The influence of the user on the evaluation of the PMV was set for each simulation assuming a metabolic rate of 1.2 met (typical for office work activity), and a thermal resistance of clothing of 0.5 clo (typical for summer season).

In Table 2, the input data obtained by the experimental campaign are summarised. Only the normal beam solar radiation (I_{bn}) was modelled, starting from the measured data of global solar irradiation on the façade.

Table 2 – Input data to evaluate the PMV during peak condition.

		Time of peak condition	ϑ_{in}	ϑ_{surf}	I_{in}	I_{bn}	τ_e
		[h]	[°C]	[°C]	[W/m^2]	[W/m^2]	[-]
DAY 7 05/07/2013	*TGU*	14:00	26.6	37.1	146	759	0.30
	TGU_TT	14:00	26.6	31.8	64	759	0.13
	TGU_TT+PCM(IN)	16:00	26.6	30.3	7	735	0.02
DAY 8 21/07/2013	*TGU*	13:00	26.8	39.2	180	800	0.30
	TGU_TT	14:00	26.7	32.6	65	745	0.15
	TGU_TT+PCM(OUT)	16:00	26.6	30.3	38	723	0.13

For each distribution of the PMV index, the amount of floor area where the PMV was within the comfort categories was evaluated. According to ISO 7730:2005 (EN, 2005), category A is obtained when the predicted percentage of dissatisfied people (PPD) is lower than 6% (PMV varying in the range ±0.2), category B relates to the condition where

the PPD is between 6% and 10% (PMV varying in the range ±0.5), and category C corresponds to a PPD of between 10% and 15% (PMV varying in the range ±0.7).

In addition, spot PMV values were calculated at a distance of 0.75 m from the window to consider the possible minimum distance of a work desk.

An important issue to note when analysing transparent building envelopes is the transmitted solar radiation. Since the PMV index does not consider this variable, in order to account for the effects of the short-wave solar radiation on the user, two modified indices were evaluated and a distance from the window of 0.75 m was considered in addition to the standard PMV index.

Firstly, the modified predicted mean vote (PMV*) (Lyons P., Arasteh D., 2000) was calculated according to Equation 6.

$$PMV^* = PMV + I_{in} \cdot 0.0024$$

Equation 6

Where I_{in} is the transmitted solar radiation.

Secondly, the methodology implemented in SolarCal (Arens et al., 2015) was applied, and another equivalent PMV index (PMV**) was assessed and compared with the PMV*.

The SolarCal model defines the additional effective radiant field (ERF) exchanged by the body with the surrounding surfaces when it is exposed to incident solar radiation. The software returns the additional mean radiant temperature (MRT) in order to evaluate a solar-adjusted MRT. Standard literature values to define the environment (floor reflectance), the geometry of the problem, the position of the user and the user's surface property (sky vault fraction, fraction of body, skin absorptivity) were used (Arens et al., 2015).

The input data used for evaluating the thermal comfort indices are reported in

Table **3**.

The local thermal discomfort was assessed considering the radiant asymmetry due to warm wall (ISO 7730:2005).

Table 3 – Input data for modelling the thermal comfort.

Relative humidity	50%
Metabolic rate	1.2 met
Thermal resistance of clothing	0.5 clo

Air velocity	0.1 m/s
User position	seated
Sky vault view fraction	0.2
Fraction of the body	0.5
Average short-wave absorptivity	0.67
Floor reflectance	0.4

3. Results

3.1 Solar properties

3.1.1 Solar transmission coefficient

The solar transmission coefficient (τ_e) evaluated for the reference technology (TGU) was in the range 0.3–0.4; a range is provided because the values of impinging/transmitted solar irradiance used in the calculations were characterised by different beam angles.

With regard to the triple glazing unit with thermotropic glazing (TGU_TT), the methodology explained in 2.2.1 paragraph was applied. The solar transmission coefficient of TGU_TT as a function of the external surface temperature and the corresponding double-change-point fit are represented in Figure 5, and the regression coefficients that guaranteed the best overall fit of the experimental data (with an RMSE of 0.02) are reported in Table 4. The changes in solar transmission coefficient occurred when the external surface temperature of the glazing ranged between 17.1 °C and 33.8 °C. The resulting transitions occurred at lower temperatures than the nominal range of 20 °C to 40 °C declared by the manufacturer. Therefore, both the temperature range of the transition and the difference between the solar transmission coefficients in *on* and *off* states were smaller than the nominal values. Solar transmission values of 0.19 and 0.14 were respectively estimated for *off* and *on* states. Of course, these values are much lower than those for the TT only (0.45 and 0.36 respectively in *off* and *on* state (Bianco et al., 2015)) due to the combined presence of the TGU. However, a much smaller variation between *on* and *off* states was observed for the field-based measurements.

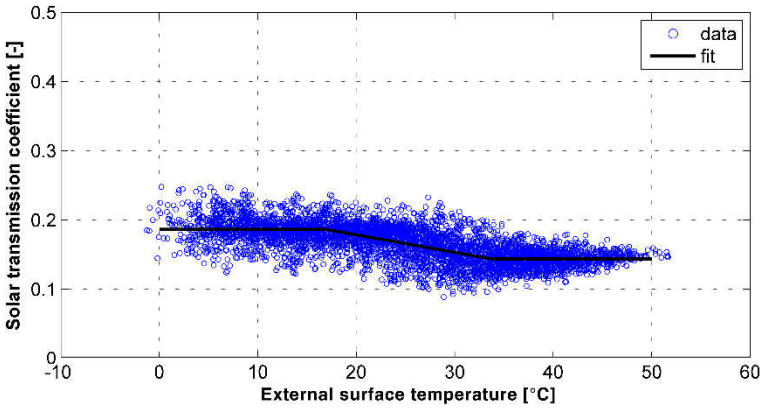

Figure 5 – Solar transmission coefficient of the TGU_TT as a function of the external surface temperature.

Table 4 – Regression coefficients of the solar transmission coefficient of the TGU_TT.

$\tau_{s,off}$	ϑ_{off}	β_2	ϑ_{on}	$\tau_{s,on}$
0.19	17.1	-0.0025	33.8	0.14

The solar transmission coefficient, assessed as a function of the external surface temperature of the glazing, for the dynamic TGU_TT+PCM technologies is reported in Figure 6. The TGU_TT+PCM(IN) component presented a stable value of solar transmission of around 0.02. Contrastingly, the solar transmission of TGU_TT+PCM(OUT) increased with the external surface temperature; a solar transmission of about 0.05 was obtained for temperatures between 20 °C and 35 °C. A considerable increase in the solar transmission (up to about 0.18) was observed for external surface temperatures higher than 35 °C, when the PCM in the outer cavity was completely melted.

It should be noted that the external surface temperature can be representative of the PCM's temperature only for the TGU_TT+PCM(OUT) configuration. When the PCM was placed in the innermost cavity, its temperature was close to that of the ambient air. However, the comparison of the solar transmission as a function of the external surface temperature highlights that when the PCM was placed in the innermost cavity, it did not change phase, regardless of the outdoor temperature.

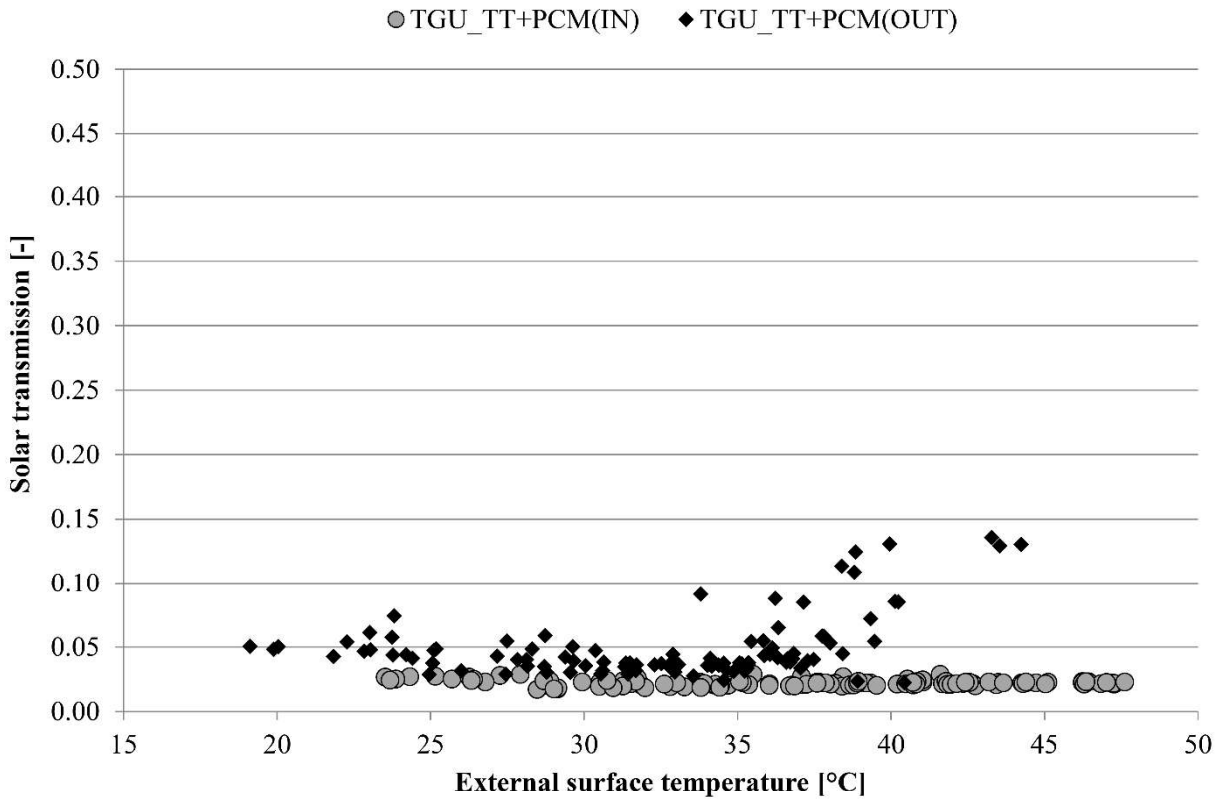

Figure 6 – Solar transmission coefficient as a function of the external surface temperature, TGU_TT+PCM(IN) and TGU_TT+PCM(OUT).

3.1.2 Equivalent solar factor

The daily trend of the equivalent solar factor (calculated with Equation 2 and the methodology presented in paragraph 2.2.2) is reported in Figure 7. For the reference technology (TGU), an average value for *g*-value* of 0.46 was obtained. As expected, this value is lower than the theoretically calculated value of *g-value*, which was 0.60 (Table 3 in Bianco et al., (2017)).

For the TGU_TT technology, a quite stable value for *g*-value* of around 0.20 was evaluated from the measured data. In line with the TGU, this value is also lower than the theoretically calculated values for *g-value* of 0.32 and 0.27, respectively, for the *off* and *on* states (Table 3 in Bianco et al., (2017)). Since the equivalent solar factor is a daily average value, the difference between the *on* and *off* states of the thermotropic layer could not be detected with this simplified methodology.

In responsive glazing systems with PCM, low values of equivalent solar factor are associated with low energy transmission through the glazing. Therefore, it can be stated that low values of *g*-value* were calculated for days when the PCM remained solid, whereas higher values occurred when the PCM melted, whence a greater amount of solar radiation could enter the indoor environment. In general, *g*-value* calculated for TGU_TT+PCM(OUT) (Figure 7, from

Day 16 to 30) tended to present higher values than those of the TGU_TT+PCM(IN) (Figure 7, from Day 1 to 15). The TGU_TT+PCM(IN) component presented a quite uniform trend, with *g*-value* ranging between 0.05 and 0.07. As could be inferred from the resulting solar transmission coefficient in Figure 6, the PCM placed in the inner cavity did not change phase during the selected days. For this reason, TGU_TT+PCM(IN) maintained a low equivalent solar coefficient during the analysed summer days, drastically reducing the solar heat gains when compared to the TGU_TT (i.e. *g*-value* was 0.06 versus 0.20).

In comparison, the equivalent solar factor of TGU_TT+PCM(OUT) presented a wider variety of values over the period of analysis, ranging from 0.02 to 0.14. Low values of *g*-value* for TGU_TT+PCM(OUT) were calculated during the days 16–21, when the glazing had just been rotated to place the PCM from the inner to the outer cavity of the responsive glazing, and therefore it was solid. Moreover, the boundary conditions presented a drop in the average outdoor air temperature, and the solar radiation was not particularly high. Subsequently, as the temperatures increased again, the PCM underwent the melting process, and the equivalent solar factor increased. On Day 26, which was characterised by high outdoor air temperature but low solar irradiation, the corresponding value of *g*-value* was in line with those of the previous days. It can be inferred that the glazing is affected by a memory effect. Although the highest solar radiation among the selected period occurred on Day 29, the equivalent solar factor of TGU_TT+PCM(OUT) noticeably decreased due to a drop in the outdoor air temperature. Therefore, during the summer season, when the peak of the solar radiation on a south-exposed façade is lower than in winter, the resulting *g*-value* will be mostly influenced by the outdoor air temperature.

To summarise, it can be stated that the position of the PCM in the cavity modifies the solar gain of the responsive glazing system. When the PCM is positioned in the inner cavity, no particular variation during the day is noticed, meaning that the PCM remains solid. However, if the PCM is positioned in the outer cavity, a variation in *g*-value* (according to the boundary conditions) is noticed, and shows particular dependency on the outdoor air temperature.

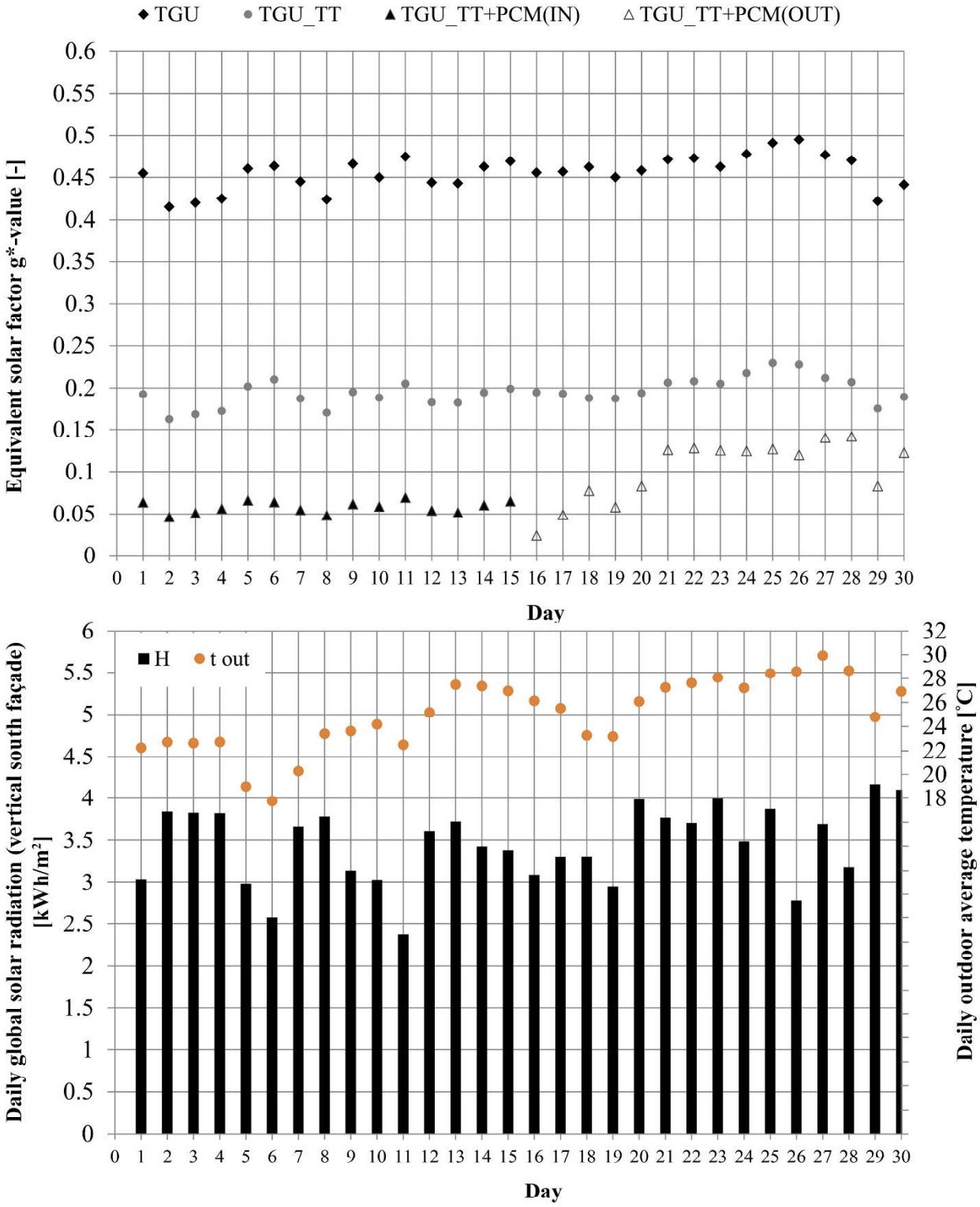

Figure 7 – Equivalent solar factor of the three technologies and boundary conditions.

3.2 Daily analyses

3.2.1 Cloudy days

The measured values of surface heat flux, external surface temperature, transmitted solar radiation and total surface heat flux during cloudy summer days (Day 5 and Day 6) are reported in Figure 8. As with the behaviour observed in winter (Bianco et al., 2017), during the night, the surface heat flux through the four technologies were almost the same. During daytime, the surface heat flux through TGU_TT and TGU_TT+PCM(IN) were very similar during Day 5, as well as being similar through TGU_TT and TGU_TT+PCM(OUT) during Day 6 (Figure 8a). This similarity between the behaviour of the technologies with and without PCM hints at a lack of phase transition of the PCM layer. The surface heat flux through TGU_TT and TGU_TT+PCM ranged from -5 to +5 W/m^2, whereas higher values were registered for the reference technology (TGU). During Day 6, the heat flow of the three technologies dropped at 15:00 due to a sudden reduction in the solar radiation. This provides a further indication that phase transition of the PCM during cloudy days did not occur, as the TGU_TT+PCM did not show a significantly increased thermal inertia (this will be more evident from the discussion of the sunny days in paragraph 4.2.2). The external surface temperature (Figure 8b) shows a peak value of around 27 °C during both Day 5 and Day 6. The transmitted solar radiation (Figure 8c) was lower than 20 W/m^2 for the technologies with PCM in both positions. Due to the low solar energy incident on the façade, it can be asserted that the PCM remained solid. The thermotropic glazing was able to halve the solar radiation through the component, when compared to the reference.

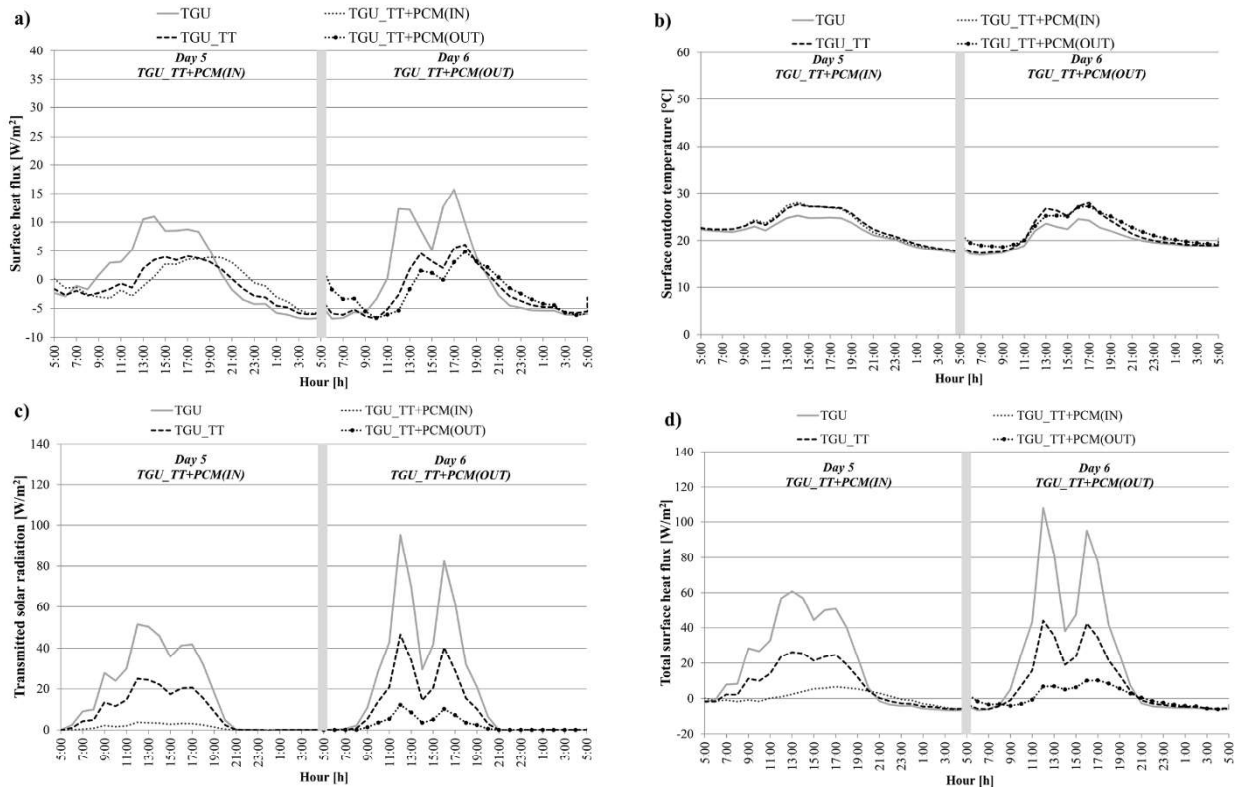

Figure 8 – Day 5 and Day 6 (cloudy days): a) surface heat flux, b) external surface temperature, c) transmitted solar radiation and d) total surface heat flux.

The daily total energies entering through the technologies are reported in Figure 9. During Day 5 and Day 6, no significant difference is noticeable for the analysed configurations. As expected, the highest energy values were found for the reference technology (TGU), for which 445 Wh/m^2 and 527 Wh/m^2 were observed on Day 5 and Day 6, respectively. The energy entering through the TGU_TT technology was 183 Wh/m^2 for Day 5 and 207 Wh/m^2 for Day 6; a reduction of about 60% compared to the reference. Regardless of the PCM's position, a very low energy gain, between 13 Wh/m^2 and 15 Wh/m^2, was observed through the TGU_TT+PCM glazing systems.

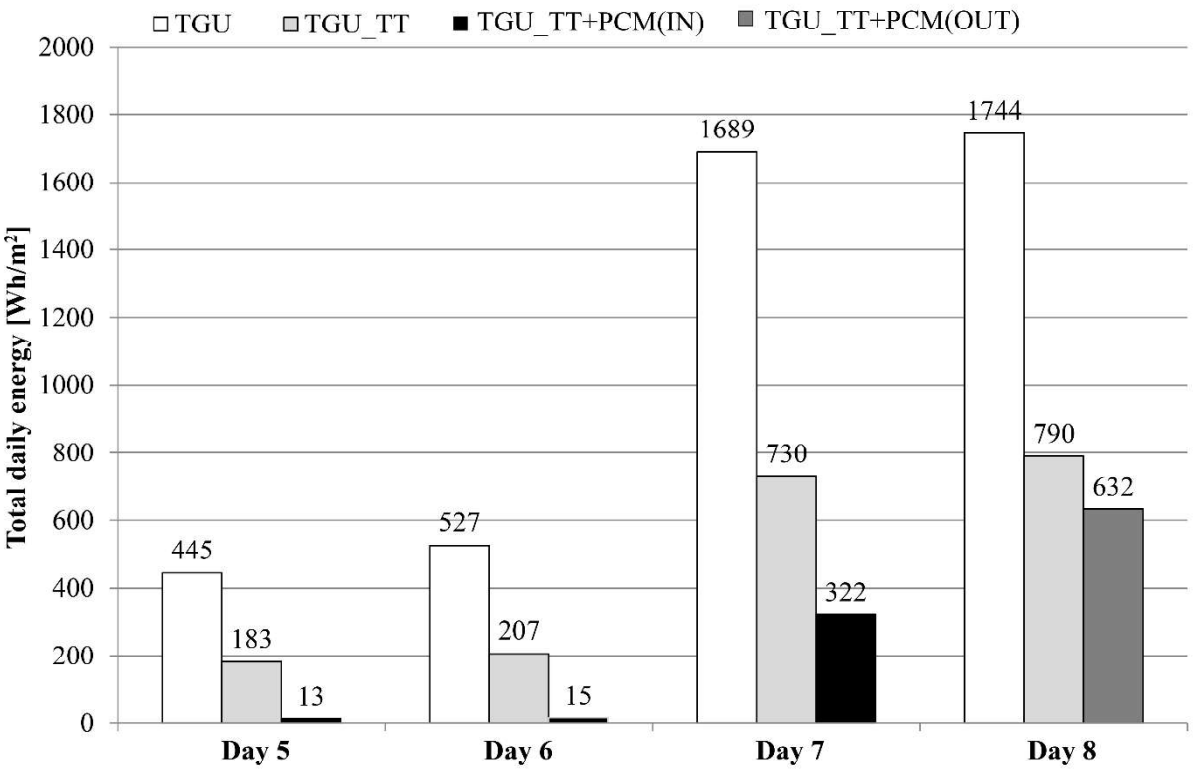

Figure 9 – Daily total energy gains.

3.2.2 Sunny days

The results for Day 7 and Day 8 are reported in Figure 10. The trend of the surface heat flux through the reference technology was similar to that of a bell curve that follows the incident solar radiation. The TGU peaks occurred at 13:00 and 14:00, for Day 7 and Day 8, respectively with values around 90 W/m^2. With regard to the TGU_TT technology, the monitored surface heat flux values were almost the same during Day 7 and Day 8. The peak value was slightly higher than 30 W/m^2, and it occurred at 15:00 (Figure 10a). The presence of the thermotropic layer allowed a reduction in surface heat flux of about one third of the reference TGU, and delayed the peak by approximately 2 hours. With regard to the TGU_TT+PCM, the adoption of the PCM layer increased the peak shift even further (up to 4 hours), regardless of

the PCM's position. However, in presence of high solar radiation, the position of the PCM had an influence on the thermal performance of the systems. In the case of TGU_TT+PCM(IN), the trend of the surface heat flux was similar to that of TGU_TT, hinting at a lack of phase transition of the PCM layer, or at least an incomplete transition. TGU_TT+PCM(OUT), however, showed a different behaviour during both day and night, with a constant heat flux of about 10 W/m^2 for the whole day with the exception of the central hours. The small bell shape characterising the heat flux curve in the middle of the day can be explained by the melting of the PCM (which can be inferred also by the gradual increase in the transmitted solar radiation). The steady value during the night hours can be related to the solidification phase of the PCM, whereas during the morning, the latent heat of fusion was exploited until complete melting occurred.

With regard to the transmitted solar radiation, the reference technology showed peak values at 13:00 of 160 W/m^2 and 180 W/m^2 respectively for Day 7 and Day 8. The thermotropic glazing lowered the peak of solar radiation transmitted through the component TGU_TT by 60%, compared to the reference TGU during both days (69 W/m^2 and 79 W/m^2 for Day 7 and Day 8, respectively).

Very little solar radiation passed through when the PCM was placed in the inner cavity, whereas a higher solar radiation was transmitted when the PCM was in the outer cavity (Figure 10c). For TGU_TT+PCM(IN), the maximum solar transmission was only 11 W/m^2, measured at 13:00, as the PCM did not undergo phase transition and remained opaque. For TGU_TT+PCM(OUT), the maximum solar transmission (53 W/m^2) occurred at around 15:00, when the PCM was melted and its solar transmission coefficient had therefore increased, allowing for the transmission of a larger amount of solar radiation. During Day 8, a drop of the solar radiation was registered at around 14:00. At that time, a reduction of heat flux for TGU and TGU_TT was registered, whereas the behaviour of the TGU_TT+PCM (OUT) was not influenced due to the increased thermal inertia provided by the PCM. The total heat fluxes are reported in Figure 10d. The lowest values of total heat flux can be observed when the PCM is in the inner cavity.

Figure 10b shows the trend of the external surface temperature. The highest value (50.2 °C) was reached by the TGU_TT during Day 7. Slightly lower temperatures were monitored for TGU_TT+PCM(IN) and the reference. During Day 8, however, the TGU_TT+PCM(OUT) case presented a different trend. Due to the phase transition of the PCM, the peak surface temperature was reached one hour later than for the other two technologies. Furthermore, during the late hours of the afternoon, the surface temperature was higher than that of the TGU and TGU_TT due to the solidification phase and the release of the heat stored during the day. This difference between the behaviour of TGU_TT+PCM(OUT) and TGU_TT+PCM(IN) further supports the view that phase transition occurred only when the PCM was placed in the outer cavity.

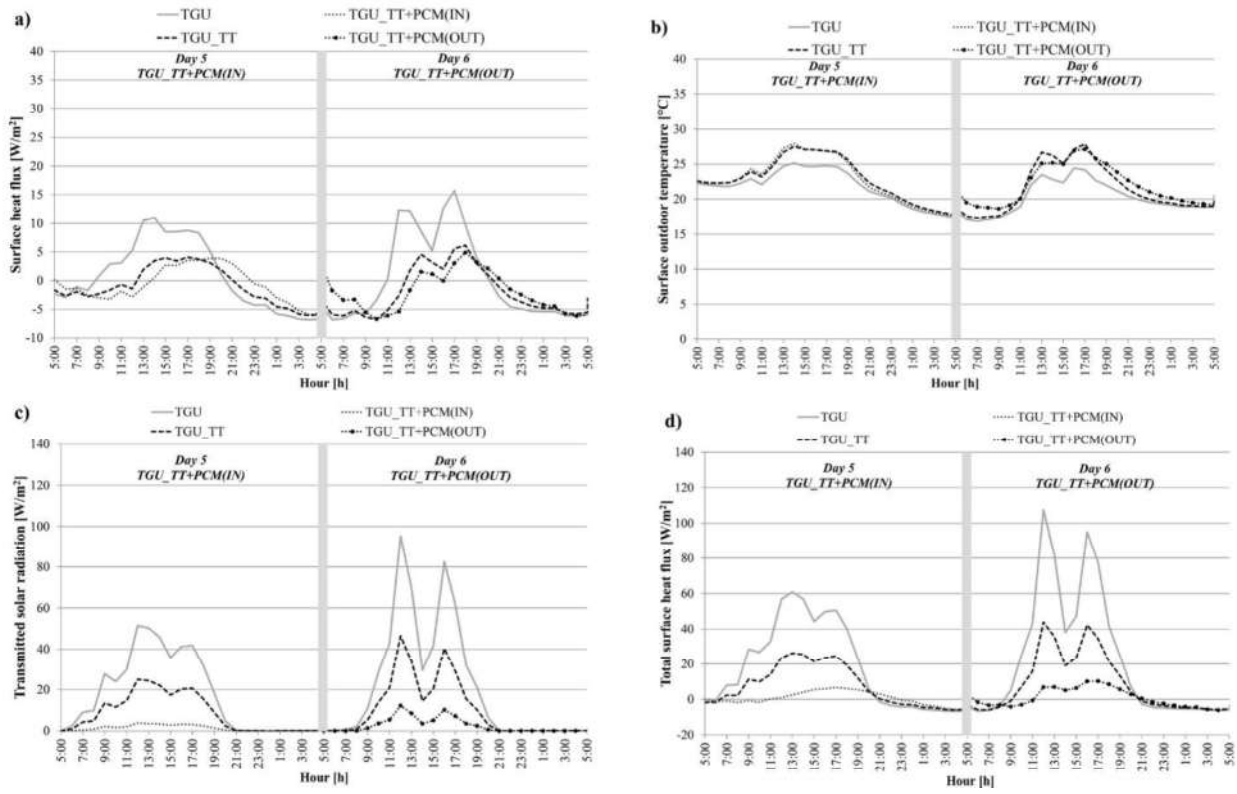

Figure 10 – Day 7 and Day 8 (sunny days): a) surface heat flux, b) external surface temperature, c) transmitted solar radiation and d) total surface heat flux.

The daily total energies evaluated for the reference technology (TGU) were 1689 Wh/m^2 and 1744 Wh/m^2, during Day 7 and Day 8, respectively (shown on Figure 9), whereas values of 730 Wh/m^2 and 790 Wh/m^2 were calculated during Day 7 and Day 8 for TGU_TT. The integration of the thermotropic layer in the triple glazing unit reduced the energy transmitted through the technology by more than half (-57% and -55%) when compared with the reference TGU.

By analysing the total energy, the strong performance of the TGU_TT+PCM can be confirmed. The lowest transmitted energy was calculated for TGU_TT+PCM(IN) during Day 7 (322 Wh/m^2), whereas TGU_TT+PCM(OUT) showed a much higher transmitted energy value during Day 8 (632 Wh/m^2). The contribution of the PCM can be inferred by comparing TGU_TT+PCM and TGU_TT; the reduction in terms of total energy was estimated to be 56% during Day 7 for TGU_TT+PCM(IN) and a 20% reduction during Day 8 for TGU_TT+PCM(OUT).

3.3 Long-term energy performance

Daily positive peak total heat flux are plotted in Figure 11 and Figure 12, respectively, for the sets with the PCM positioned in the inner and outer cavity. TGU_TT+PCM(IN) presented peak values of total heat flux ranging between 8 W/m^2 and 33 W/m^2 (Figure 11), whereas for TGU_TT+PCM(OUT) the range was wider; between 10 W/m^2 and 115 W/m^2 (Figure 12). The same difference between the two periods was observed also for TGU and TGU_TT. This

difference is due to the fact that globally the two periods were similar, but the boundary conditions during some of the 21 days with the PCM positioned in the outer cavity were characterised by higher values of temperature and solar radiation compared to the set with PCM in the inner cavity (see also Figure 1b and paragraph 2.2.4). However, the two figures enable synthetic visualisation of the behaviour of the responsive windows (TGU_TT and TGU_TT+PCM(IN/OUT)) during peak conditions in comparison to a standard technology (TGU). The lowest total heat flux values were measured for the two technologies with PCM (TGU_TT+PCM(IN/OUT)). With regard to TGU_TT+PCM(OUT), between Day 14 and Day 16, the peak total heat fluxes were similar to those of TGU_TT, implying that the PCM was melted.

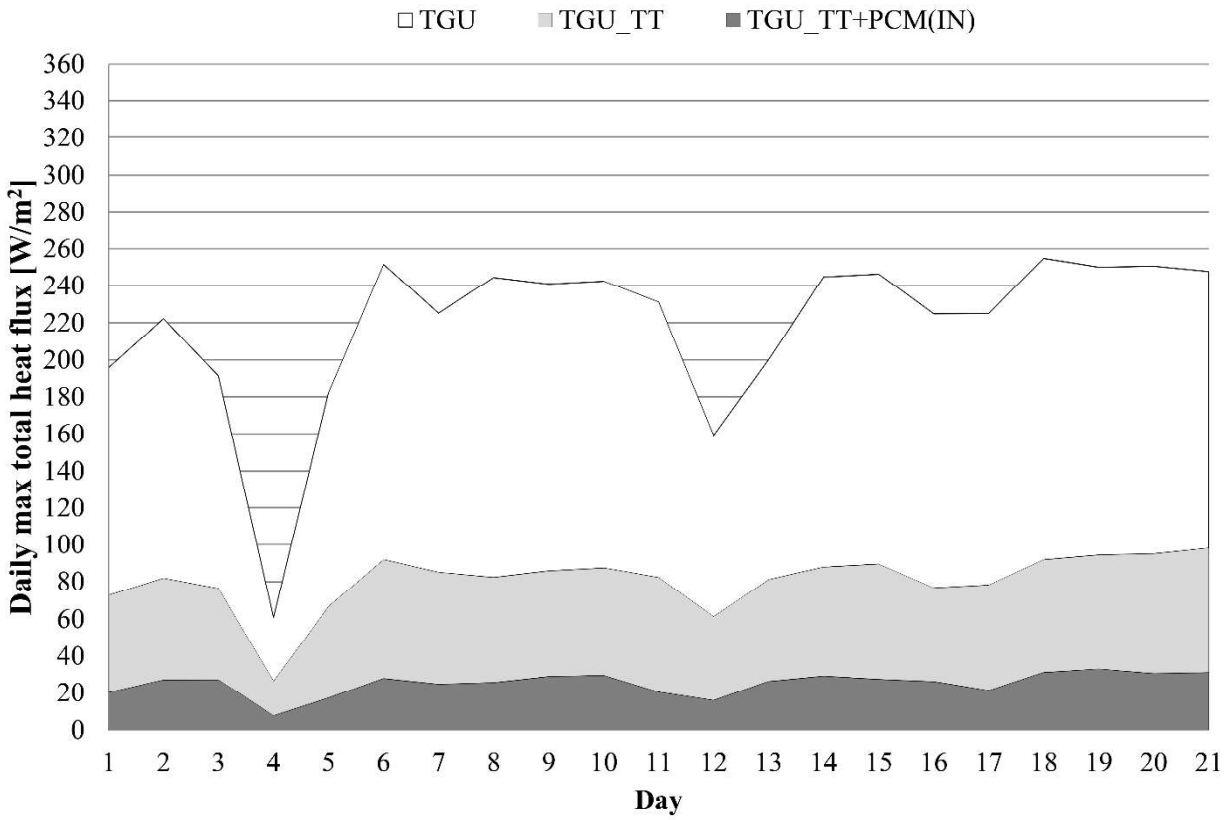

Figure 11 – Daily positive peak heat flux for the configuration with PCM in the inner cavity.

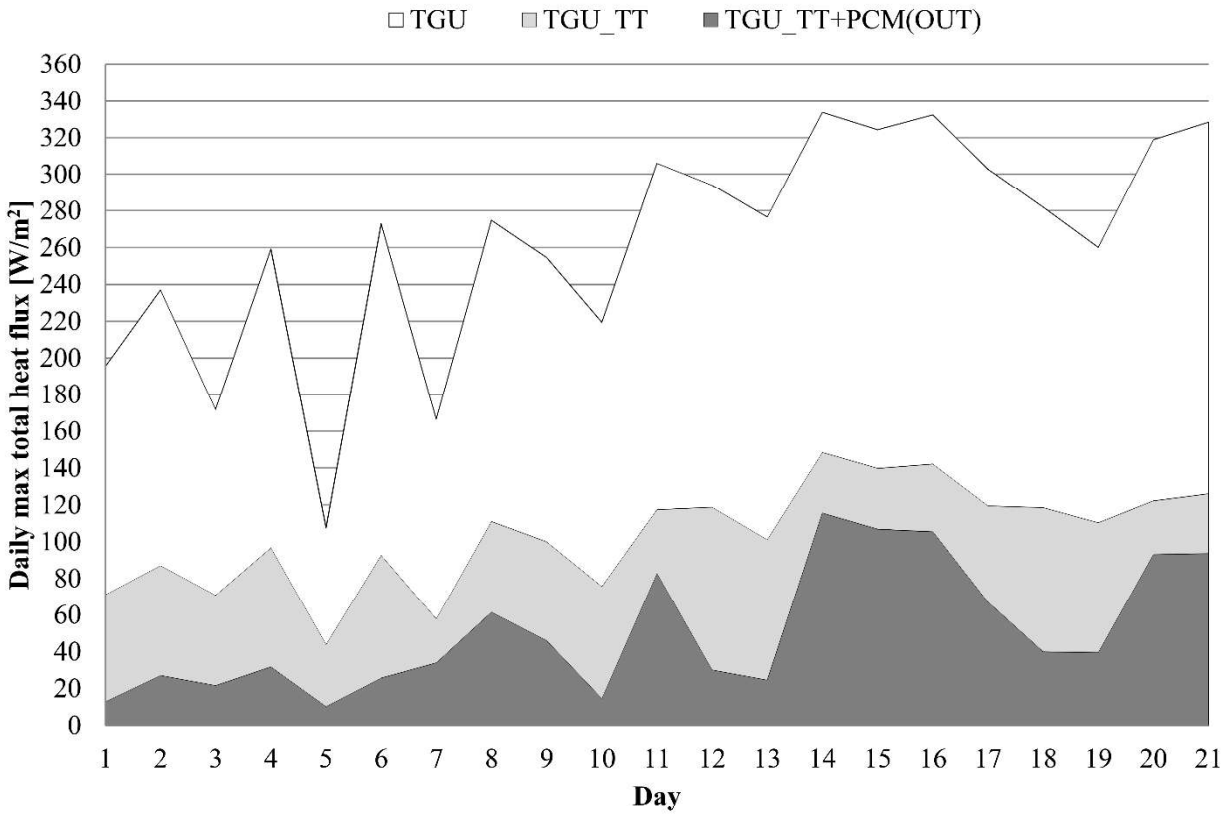

Figure 12 –Daily positive peak heat flux for the configuration with PCM in the outer cavity.

The normalised energy values are reported in Figure 13. A small difference between the two periods can be observed, as the normalised energies for the TGU and TGU_TT technologies were not exactly the same. Despite the normalisation process, the energies were approximately 10% higher during the second period, when TGU_TT+PCM(OUT) was monitored. However, this small difference is definitely within the range of the accuracy of the measurement and calculation process, and is a sign of the meaningfulness of the normalisation process, as well as of the measurement quality, and it therefore provides a solid basis for a robust comparison between the different configurations of the TGU_TT+PCM (IN and OUT). For the reference technology, normalised energy values of 679 Wh/m^{2}CDD and 730 Wh/m^{2}CDD were calculated over the two periods, whereas the TGU_TT presented values of 283 Wh/m^{2}CDD and 317 Wh/m^{2}CDD. The presence of the thermotropic layer reduced the energy by 56–58%, when compared to the reference. The lowest normalised energy (102 Wh/m^{2}CDD) was found for the TGU_TT+PCM(IN), while a corresponding value of 192 Wh/m^{2}CDD was calculated for TGU_TT+PCM(OUT). Although there is a small discrepancy between the boundary conditions of the two periods, TGU_TT+PCM(IN) presented a better performance than TGU_TT+PCM(OUT), as the normalised energy for the technology with PCM in the inner cavity was approximately 47% lower than that seen when the PCM is in the outer cavity. If the comparison is carried out between the technologies with PCM and the TGU_TT, a reduction of 64% and of 39% was obtained for the PCM in the inner and outer position, respectively. As a general comment, it is important to underline that the energy reduction was mostly

due to the thermotropic layer. The integration of PCM allowed for further improvements to the glazing system's performance, especially when the PCM was placed in the inner cavity.

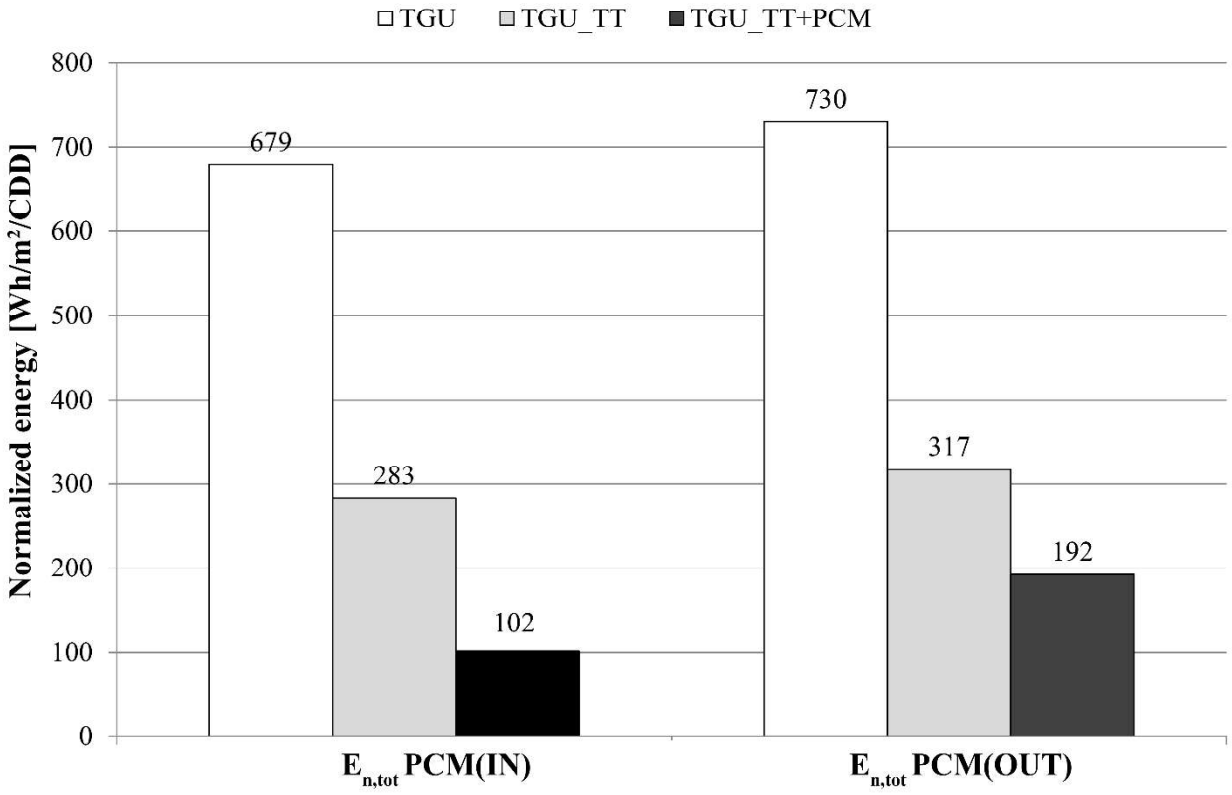

Figure 13 – Normalised total energy over two periods.

3.4 Thermal comfort performance

The input data (coming from the monitoring activity) for the thermal comfort analyses are reported in Table 2, where the PMV values have been found from simulations. It can be observed that the peaks of the surface internal temperature for the three technologies do not coincide (Figure 14). The technology with PCM, presented a delay of 2 and 3 hours for Day 7 and Day 8, respectively, when compared to the reference technology (TGU), whereas the glazing with the thermotropic layer presented a delay of one hour. For this reason, the analyses were conducted at 13:00 for the TGU, at 14:00 for TGU_TT and at 16:00 for TGU_TT+PCM (both for IN and OUT position of the PCM), in order to represent the peak condition.

In Figure 15, the floor distributions of the PMV during Day 7 and Day 8 are represented. The results of the comfort evaluations are also reported in Table 5. Considering the south façade to be entirely glazed, none of the technologies allowed category A conditions to be reached during the peak hours. The largest part of the floor area fell into category B for all the glazing technologies.

Close to the façade, portions of floor area in discomfort were found both with TGU and TGU_TT (21% and 7% during Day 7, and 24% and 11% during Day 8), but not with the TGU_TT+PCM (even though 22% of the floor area fell into category C during both Day 7 and Day 8). The insertion of the PCM in the cavity of the triple glazing unit could, therefore, improve the thermal comfort conditions. The thermotropic layer was also capable of reducing the portion of floor area in discomfort compared to the reference.

The results of the spot evaluations of PMV, PMV* and PMV** are reported in Table 5. During Day 7, PMV values of 0.61, 0.69 and 0.99 were obtained for TGU_TT+PCM(IN), TGU_TT and TGU, respectively. The TGU_TT+PCM(IN) showed the closest value to neutrality while the highest value, corresponding to a slightly warm sensation, occurred with the reference technology. Due to the very low level of solar radiation transmitted by the TGU_TT+PCM (IN), with this technology the value of PMV* index (0.63) was very similar to that of PMV (0.61). Consequently, the positive impact of glazed technologies integrating PCMs is most pronounced when there is high solar radiation. Contrastingly, PMV* was 0.84 and 1.34 for TGU_TT and TGU, respectively, hence both technologies led to discomfort conditions when considering this modified index. Higher values of equivalent PMV (PMV**) were found, following the methodology presented in (Arens et al., 2015).

Analysing the results of Day 8, similar considerations can be obtained. Since the peak surface temperatures were equivalent, the PMV evaluated for TGU_TT+PCM(OUT) was the same as that of TGU_TT+PCM(IN). It could therefore be inferred that the position of the PCM did not affect the thermal comfort. However, considering that the boundary conditions of Day 8 were slightly worse than Day 7, it can be deduced that, in terms of traditional PMV, the thermal comfort performance of TGU_TT+PCM(OUT) was slightly better than that of TGU_TT+PCM(IN). On the other hand, when considering the effect of the solar radiation impinging on the occupants, TGU_TT+PCM(IN) outperformed TGU_TT+PCM(OUT), with a PMV* and PMV** of 0.63 and 0.67, respectively, compared to 0.70 and 0.93 with TGU_TT+PCM(OUT).

In general, it is possible to state that the equivalent PMV** is always higher than the PMV* assessed with the simplified relation in Equation 6. Analysing the difference between the two values, it can be seen that the PMV** is more sensitive to solar radiation.

With regard to the local thermal discomfort, the highest radiant temperature asymmetry occurred during the peak hours of the surface internal temperature. Since the radiant temperature asymmetry was well below 23 °C (EN, 2005), the internal surface temperature of the three glazing systems did not present a risk of local discomfort.

The thermal comfort results obtained can be compared to those of a previous work, where the integration of the PCM in a double glazing unit was investigated (Goia et al., 2013). Some criticalities and discomfort conditions were previously reported when the PCM was completely melted, because higher indoor surface temperatures were found. Discomfort conditions never occurred with the adoption of the TGU_TT+PCM, which means that the new prototypes of responsive glazing were able to further improve thermal comfort during the cooling season.

Table 5 – Results of the comfort evaluations during peak conditions: percentage of the floor area distribution in each comfort category; PMV, PMV and PMV** at a distance of 0.75 m from the window.*

Day 7		*TGU_TT+PCM(IN)*	*TGU_TT*	*TGU*
Category B	$0.2 < PMV \leq 0.5$	78%	74%	66%
Category C	$0.5 < PMV \leq 0.7$	22%	19%	12%
Discomfort	$PMV > 0.7$	0%	7%	21%
PMV (0.75 m)		0.61	0.69	0.99
PMV* (0.75 m)		0.63	0.84	1.34
PMV** (0.75 m)		0.67	1.03	1.83
Day 8		*TGU_TT+PCM(OUT)*	*TGU_TT*	*TGU*
Category B	$0.2 < PMV \leq 0.5$	78%	72%	65%
Category C	$0.5 < PMV \leq 0.7$	22%	17%	11%
Discomfort	$PMV > 0.7$	0%	11%	24%
PMV (0.75 m)		0.61	0.69	0.99
PMV* (0.75 m)		0.70	0.85	1.42
PMV** (0.75 m)		0.93	1.08	1.87

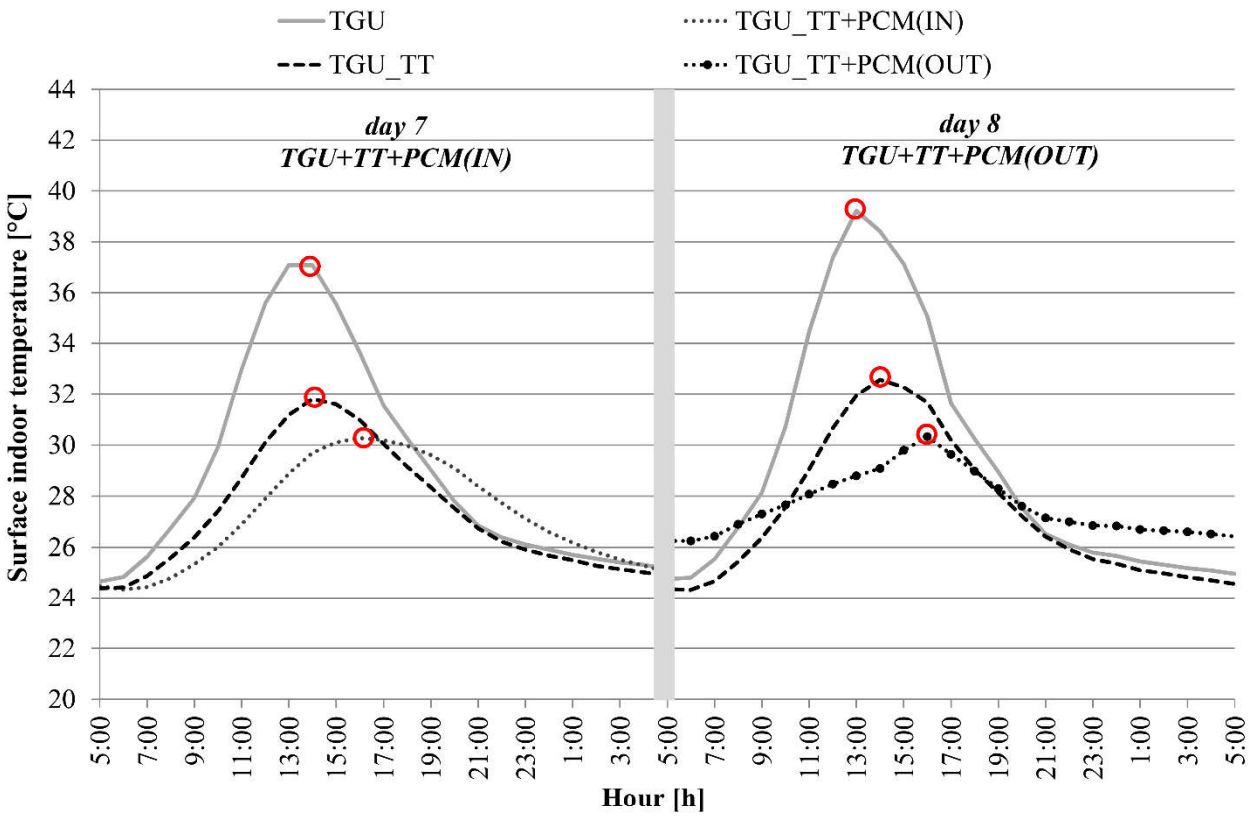

Figure 14 – Internal surface temperatures during Day 7 and Day 8.

Day 7

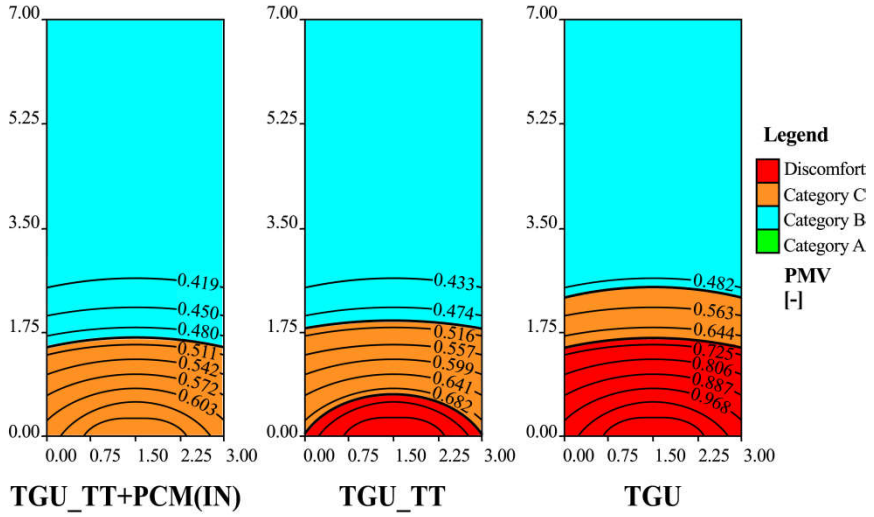

Day 8

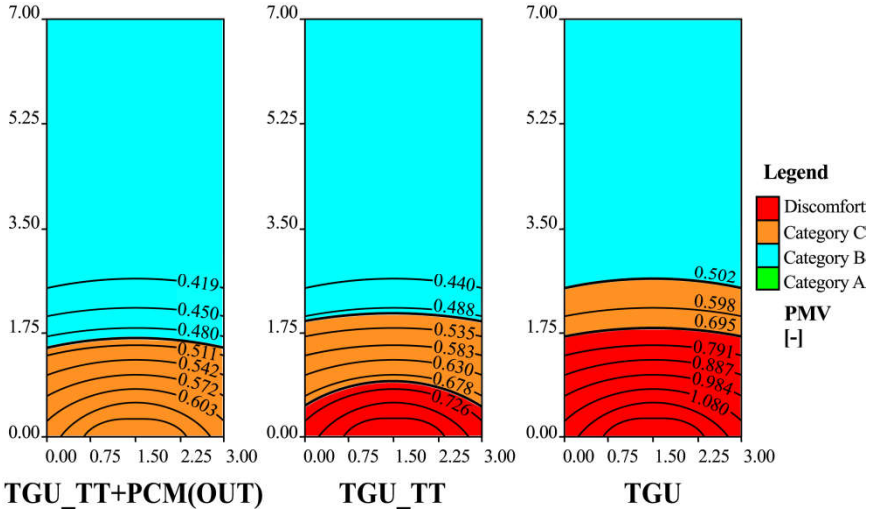

Figure 15 – Floor distribution of the PMV values during Day 7 and Day 8.

4. Discussion

4.1 Conventional metrics

The performance characterisation of the three responsive glazing systems (the two TGU_TT+PCM systems and the TGU_TT) and of the reference technology (TGU) has led to the determination of conventional metrics that are representative of systems with no dynamic behaviour and that are under steady-state conditions. The thermal transmittance of each system has been characterised during the winter season because of the better experimental conditions (larger temperature difference between indoor and outdoor air) and the better match with the underpinning assumption necessary to define the U-value of a technology (steady-state heat transfer). The insertion of a PCM layer in place of an "empty" (air-filled) cavity does not substantially impair the good thermal resistance performance of the

system, and results in an increase in the (equivalent) thermal transmittance of approximately 10%. A relevant increase in the thermal transmittance was previously verified for a case of a double glazing unit filled with PCM (Goia et al., 2014b). However, in the case of a triple glazed layout, it seems that having just one of the two cavities filled with air (and coupled to a low-emissivity coating) is enough to assure a satisfactory thermal resistance to the assembly. This makes it possible to use the second cavity to host the PCM (which also contributes to a low thermal transmittance, thanks to its relatively low thermal conductivity) without impairing the overall thermal resistance of the triple glazed system.

Under winter conditions, the optical and solar properties of the studied glazing – a triple glazing with thermotropic glass and PCM (TGU_TT+PCM) – showed an interesting range of dynamicity during sunny winter days. The solar transmittance varied between 0.01 to 0.03 for a solid PCM condition, for both TGU_TT+PCM(IN) and TGU_TT+PCM(OUT), and up to 0.17 for melted PCM (a condition occurring only when the PCM is hosted on the outermost cavity). Under summer conditions, the TGU_TT+PCM(IN) system again showed a stable value of solar transmission of around 0.02, in line, therefore, with the winter behaviour. Contrastingly, the solar transmission of TGU_TT+PCM(OUT) increased as the external surface temperature increased, with a solar transmission of about 0.05 found in the temperature range of 20 °C to 35 °C, and up to 0.18 when the external surface exceeded 35 °C, when the PCM in the outermost cavity was completely melted. The behaviour in fully melted and fully solid state in the summer is therefore consistent with that seen in the winter, and the geometrical features of solar radiation (different solar height) does not influence the solar transmission by itself. This fact can be explained by considering that the glazing system is highly diffusive in all its states (either because of the PCM layer when this is solid, or because of the thermotropic layer when the PCM is melted).

The equivalent solar factor of the TGU_TT+PCM(IN), whose PCM layer always remained solid, presented a quite uniform trend, with an average value over the tested period of 0.06. By way of contrast, the equivalent solar factor of the TGU_TT+PCM(OUT) showed a greater variability (ranging between 0.02 and 0.14 over the analysed period), due to the occurrence of the phase transition within the PCM layer which, during summer, was mostly driven by the outdoor air temperature. When the PCM was solid, only a small amount of the incident solar radiation was transmitted, whereas a greater amount of solar radiation was allowed to enter the indoor environment once the PCM was liquid. Therefore, even though the equivalent solar factor returns an average daily behaviour, this number can provide some indications as to the state of the glazing unit with PCM (i.e. if the PCM is melted or not). No information on the state of the glazing could be derived for the TGU_TT set (i.e. whether the TT layer was *on* or *off*), due to the low range of variation in the

behaviour of the TT layer, which could not be detected with this methodology. An average equivalent solar factor for the TGU_TT of 0.20 was obtained.

The limited effect of the TT layer in preventing the complete melting of the PCM layer can be partially attributable to the dynamic range of the thermotropic layer, which turned out to be smaller than that declared on the available technical datasheet (Bianco et al., 2015). In a previous laboratory characterisation (Bianco et al., 2015), the change in the solar transmittance for the same TT-glazed pane used in these prototypes was found to be approximately 0.10 – from a solar transmittance of 0.45 when in *off* state (around 11 °C) to 0.36 when in *on* state (around 45 °C). These results on the TT-glazed pane alone are confirmed when the technology is installed in a more complex system (a TGU) and tested in the field. During the experiment presented in this paper, solar transmission values of 0.19 and 0.14 were estimated for *off* and *on* states, respectively. These quantities are not only much lower in absolute value than those for the TT alone (Bianco et al., 2015), due to the combined presence of the TGU, but the variation range is also noticeably smaller (approximately half of that of the TT pane alone).

The analysis of the prototypes in the test cell showed that a greater dynamic range is necessary to control the charging phase of the PCM when it is installed in the outermost cavity. The aim of a glazing configuration coupling PCM and TT layers is that the thermotropic (dynamic) layer offers shielding of the PCM (dynamic) layer from the solar radiation when the PCM layer is reaching full transition, so that it remains in the transition phase. The TT layer is very promising because of the intrinsic features that make it very suitable to be coupled with a PCM layer. The switch in the optical properties of the selected thermotropic glass occurs because of the phase transition of a paraffin wax mixture contained in the core of particles dispersed within a polymer layer (Bianco et al., 2017). It is therefore possible to adjust the temperature range in which the optical properties change by choosing a different paraffin wax mixture (a different PCM itself) for the core of the particles of the thermotropic layer. The two PCM substances (the one inside the TT layer and the bulk one in the TGU's cavity) can therefore be selected to work together within the same range of temperature. However, it became clear during the experimental assessment that the range of dynamicity of the TT technology is not sufficient to achieve the desired overall behaviour of the system when the PCM is placed in the outermost cavity.

4.2 Daily analyses and long-term performance

The analysis of the systems' behaviour not only focused on conventional performance metrics, but also included short-term (daily) assessments on specific peak conditions, and long-term (using approximately three weeks for each season) performance analyses. Table 6 summarises the results for winter and summer seasons; for more details, refer to Figure 9.

Daily total energy analyses (Table 6) conducted in the summer season show that:

- The heat gain through the TGU_TT+PCM is approximately 3% of that of the reference TGU (and approximately 40% of that of the reference TGU_TT) under a cloudy sky condition, regardless of the position of the PCM layer (innermost or outermost cavity);
- The heat gain through the TGU_TT+PCM under sunny sky conditions depends on the position of the PCM layer, and is approximately 20% of that through the reference TGU when the PCM is in the innermost cavity (TGU_TT+PCM(IN)), and it rises up to approximately 35% of that through the reference TGU when the PCM is in the outermost cavity (TGU_TT+PCM(OUT)); and
- The TGU_TT system presents a quite stable performance regardless of the boundary conditions, with heat gains in the range of 40% to 45% of that through the reference TGU.

In winter season, the daily total energy analyses (Table 6) show that:

- The systems with thermotropic and PCM layers (TGU_TT+PCM) have an increased heat loss compared to the reference technology TGU (+70% for TGU_TT+PCM(IN), and +80% for TGU_TT+PCM(OUT)). The thermal transmittance of the responsive glazing with PCM results in an increase of the (equivalent) thermal transmittance of approximately 10% compared to the TGU (refer to 5.1, Conventional metrics). This result is due to negative energy losses that are not counterbalanced by solar heat gains. (For more details refer to Figure 11 in Bianco et al. (2017));
- The two prototypes with TT and PCM greatly reduce the heat gain under sunny sky conditions, and these are equivalent to approximately 8% and 15% of the heat gain through the reference TGU, for the TGU_TT+PCM(IN) and the TGU_TT+PCM(OUT), respectively; and
- The prototype with TT technology only presents slightly increased total heat loss, in the range +25% to +30% compared to the reference TGU, under cloudy conditions (due to the reduction in solar heat gain), and reduced heat gain (being approximately 40% of the heat gain of the reference TGU) under sunny sky conditions. (For more details, refer to Figure 10 in Bianco et al. (2017)).

Table 6 – Summary of the daily analyses for summer and winter seasons. Percentage difference of total daily energy referred to the reference technology (TGU).

Season	**Summer**		**Winter**	
Day type	**Cloudy**	**Sunny**	**Cloudy**	**Sunny**
Energy performance	**Heat gain**	**Heat gain**	**Heat loss**	**Heat loss**

TGU	Reference value	Reference value	Reference value	Reference value
TGU_TT+PCM(IN)	3%	20%	170%	8%
TGU_TT+PCM(OUT)	3%	35%	180%	15%
TGU_TT	40%	45%	130%	40%

In light of these results, all the responsive systems present positive results during the summer season, with the TGU_TT+PCM(IN) being the most effective configuration for reducing the heat gains. Conversely, during the winter season, none of the responsive system seem particularly suitable, as all show an increase in the heat loss when little solar radiation is available, and a reduction in the solar heat gain under sunny conditions. However, this apparent negative behaviour conveyed by the daily analysis is turned around when a longer period of time is analysed (long-term performance).

Under winter conditions, both the TGU_TT+PCM(IN) and PCM(OUT) are, over the whole period of almost 3 weeks, nearly zero transfer surfaces, i.e. total heat gain equals total heat loss, so these technologies can be considered as virtually adiabatic surfaces over a longer period, with positive influence on energy demand for space heating (provided that a large area of the building envelope is realised with these technologies). The TGU_TT system shows a reduction in the total heat transferred, and reaches a value of heat gain that is approximately 35% of that of the reference TGU. When focusing on the summer season, the strong performance of the responsive system is confirmed by the long-term performance monitoring. Both the configurations with TT and PCM noticeably reduce the total heat gain over the period of three weeks. The total heat gain goes down to a value of 15% and 25% of the reference TGU's value, for TGU_TT+PCM(IN) and TGU_TT+PCM(OUT), respectively. The TGU_TT shows slightly less promising performance, with a total heat gain value slightly higher than 40% of that of the reference TGU, confirming the results from the daily analysis.

With an overall perspective that combines the heating and cooling season, the configuration with the PCM in the innermost layer (TGU_TT+PCM(IN)) seems to be most promising, as it is the one that provides the best results in general. The configuration with the PCM in the outermost layer may show a slight advantage in sunny winter days (when the full melting of the PCM layer is seen), but this is not enough to counterbalance the worse performance under the other boundary conditions. It is also important to highlight that the TGU_TT+PCM(IN) component showed a lower dynamicity compared to TGU_TT+PCM(OUT) both during summer and winter season. In fact, the PCM positioned in the inner cavity tended to stay solid. This implies that the PCM in such conditions did not undergo full melting and

solidification cycles and its latent heat of fusion was not fully exploited. This also means that the transparency of the system was not dynamic and the component stayed in a diffused state for most of the time. It is, however, worth mentioning that these results and considerations on the performance of the technology are specific to the investigated PCM (paraffin wax with nominal melting temperature of 35 °C) under the monitored climatic conditions. Therefore, for other melting temperatures of the PCM, different results could be expected.

The TGU_TT configuration is revealed to be only slightly dynamic, with a rather constant behaviour compared to the reference TGU, which is positive for most of the conditions.

4.3 Thermal comfort performance

The results of the thermophysical and energy performance studies are confirmed by investigation of the impact of the different systems on the thermal comfort conditions of an ideal room equipped with these technologies. While, under winter conditions, none of the systems presented particular threats to occupant wellbeing, the characterisation of the summer performance reveals that one of them in particular is definitely performing better.

Compared to the reference TGU, both the systems with TT and PCM were able to shift the peak value in the time profile of the indoor-side surface temperature by 2 or 3 hours under sunny summer conditions. The solution with the TT layer alone presents instead a shift of just 1 hour. Even though none of the systems were able to assure Category A conditions, the two systems integrating PCM were, however, able to provide better results, delivering a larger area under Class B conditions. The insertion of the PCM in the triple glazing unit improved the thermal comfort and reduced the floor area in discomfort conditions compared to the reference TGU.

In general, the thermal comfort performance of the two systems with PCM (in the innermost and in the outermost cavity) is very similar, and offer the greatest level of performance. However, a closer look at the entire set of conditions reveals that the configuration with the PCM located in the innermost cavity provides the best performance, as it assures that discomfort conditions due to direct solar radiation impinging on the user are avoided, due to the missing completed phase transition of the PCM layer. This behaviour confirms once more that in an overall perspective, the configuration TGU_TT+PCM(IN) is the best-performing technology, both in terms of energy and thermal comfort performance.

These results open up for the question of whether the TT layer should be located on the outermost layer of the glazing construction, or, in the intermediate glass pane, in direct contact with the PCM layer to be placed in the innermost cavity. The main concept behind the combination of a TT and a PCM layer is that they should act together. Whether the

tested prototypes can be outperformed by a glazing configuration with a TT pane in direct contact with a PCM layer placed in the innermost cavity is still unknown.

5. Conclusion

This paper presents the results of an experimental analysis to assess the energy and thermal comfort performance of responsive glazing systems during the summer season in Turin, in the northwest of Italy (Cfa climatic conditions). These novel transparent systems combine a triple glazing unit with a PCM-filled cavity (paraffin wax with melting temperature range between 33 °C and 37 °C), placed either towards the internal or external environment, and a thermotropic pane, which is always placed as the outermost layer. A triple glazing unit with the thermotropic layer alone and a reference triple glazing unit were additionally monitored. The complete description of the technologies and of the experimental apparatus, together with the evaluation of their winter performance, was presented in a previous paper (Bianco et al., 2017).

Direct solar transmission of the glazing technologies was assessed, as well as the correlation between the solar transmission coefficient and the external surface temperature of the glazing for both TGU_TT and TGU_TT+PCM(IN/OUT). A solar transmission coefficient of 0.3–0.4 was evaluated for the reference TGU, whereas solar transmission coefficients equal to 0.19 and 0.14 were calculated for the TGU_TT in *on* and *off* states respectively. Furthermore, the monitored data were used to assess the solar transmission coefficient of the TGU_TT as a function of the external surface temperature by means of a regression method. For the TGU_TT+PCM, much smaller solar transmission coefficients were evaluated when the PCM was in solid state (0.02 and 0.05 for PCM in inner and outer position, respectively), whereas a value of 0.18 was calculated for melted PCM. A new method to evaluate a daily value of an equivalent solar factor starting from experimental data was presented in the paper. Values of equivalent solar factor equal to 0.46 and 0.20 were calculated for the TGU and TGU_TT, respectively. For the TGU_TT+PCM(IN), the equivalent solar factor varied in the range of 0.05 to 0.07, whereas for the TGU_TT+PCM(OUT) it ranged from 0.02 to 0.14. These values are in line with the fact that complete phase transition of the PCM occurred only when it was placed in the outer cavity.

The energy performance was assessed by means of both a long-term evaluation and of daily analyses during cloudy and sunny days. During cloudy days, no particular results were highlighted. The TGU_TT+PCM was characterised by the lowest heat gains, with no differences according to the PCM position. The reference TGU presented heat gains that were 60% greater than the TGU_TT. Much more interesting results were found for the sunny days when the PCM and the thermotropic layer were both active. The presence of the thermotropic layer enabled a reduction in surface heat flux of about one third compared to the reference TGU and delayed the peak by 2 hours. The adoption of the PCM layer increased this peak shift even further (up to 4 hours), regardless of the PCM's position. The integration of the

thermotropic layer in the triple glazing unit allowed a reduction in the energy transmitted through the technology of more than half (-57% and -55%) in comparison with the reference TGU.

Long-term energy performance analyses showed the behaviour of the technologies over a longer time span. Energy reduction was found to be mostly due to the thermotropic layer. The integration of PCM allowed further improvement for the glazing system, especially when the PCM was placed in the inner cavity. The contribution of the PCM was inferred by comparing TGU_TT+PCM and TGU_TT; the reduction in terms of total energy was estimated to be 56% for TGU_TT+PCM(IN) and 20% for TGU_TT+PCM(OUT).

The capability of the tested technologies to improve the indoor thermal comfort was investigated. The comfort analyses were performed both in terms of traditional predicted mean vote (PMV) and of modified PMV indices that are capable of taking into account the effect of the transmitted solar radiation impinging on the occupants. Close to the façade, portions of floor area in discomfort were found both with TGU and TGU_TT (21–24% and 7–11%, respectively), but not with the TGU_TT+PCM, even though 22% of the floor area fell into category C.

Overall, the following results can be highlighted:

- The integration of thermotropic laminated glazing into a triple glazing unit (TGU_TT) was able to reduce the cooling load through the transparent component by one third when compared to a traditional triple glazing unit (TGU).
- The position of the PCM, either in the outer or in the inner cavity of a TGU, affected the overall energy performance. The phase change occurred only when the PCM was placed in the outermost cavity, with no such transition occurring when the PCM was placed in the innermost cavity.
- The insertion of the PCM in the cavity of a reference TGU was able to enhance the thermal comfort in comparison with the adoption of a traditional triple glazing unit, in particular in presence of high solar radiation incident on the glazing.
- When evaluated in terms of traditional PMV, the thermal comfort was not affected by the PCM's position. However, when the influence of the direct solar radiation impinging on the occupant was taken into account, placing the PCM in the innermost cavity achieved the best comfort conditions.

The findings presented in this paper complement and conclude the overall evaluation of the responsive glazing technologies, whose energy performance, optical, solar and thermal comfort were characterised both during summer and winter conditions. A complete methodology to experimentally assess the behaviour of responsive glazing was discussed and presented in the paper, by using data collected during extended test cell measurement exposed to real

boundary conditions. In addition, a novel methodology to select representative days was implemented in order to perform the analysis on significant periods.

References

Allen, K., Connelly, K., Rutherford, P., Wu, Y., 2017. Smart windows—Dynamic control of building energy performance. Energy Build. 139, 535–546. doi:10.1016/j.enbuild.2016.12.093

Arens, E., Hoyt, T., Zhou, X., Huang, L., Zhang, H., Schiavon, S., 2015. Modeling the comfort effects of short-wave solar radiation indoors. Build. Environ. 88, 3–9. doi:10.1016/j.buildenv.2014.09.004

Bianco, L., 2014. Involucri trasparenti innovativi. Modellazione e sperimentazione su componenti dinamici e sistemi di facciata attivi. PhD Thesis. doi:10.6092/polito/porto/2548139

Bianco, L., Cascone, Y., Goia, F., Perino, M., Serra, V., 2017. Responsive glazing systems: Characterisation methods and winter performance. Sol. Energy 155, 372–387. doi:10.1016/j.solener.2017.06.029

Bianco, L., Goia, F., Serra, V., Zinzi, M., 2015. Thermal and Optical Properties of a Thermotropic Glass Pane: Laboratory and In-Field Characterization. Energy Procedia 78, 116–121. doi:10.1016/j.egypro.2015.11.124

EN, I., 2005. ISO 7730:2005 Ergonomics of the thermal environment -- Analytical determination and interpretation of thermal comfort using calculation of the PMV and PPD indices and local thermal comfort criteria.

Favoino, F., Overend, M., Jin, Q., 2015. The optimal thermo-optical properties and energy saving potential of adaptive glazing technologies. Appl. Energy 156, 1–15. doi:10.1016/j.apenergy.2015.05.065

Giovannini, L., Goia, F., Verso, V.R.M.L., Serra, V., 2017. Phase Change Materials in Glazing: Implications on Light Distribution and Visual Comfort. Preliminary Results. Energy Procedia 111, 357–366. doi:10.1016/j.egypro.2017.03.197

Goia, F., 2012. Thermo-physical behaviour and energy performance assessment of PCM glazing system configurations: A numerical analysis. Front. Archit. Res. 1, 341–347. doi:10.1016/j.foar.2012.10.002

Goia, F., Bianco, L., Cascone, Y., Perino, M., Serra, V., 2014a. Experimental Analysis of an Advanced Dynamic Glazing Prototype Integrating PCM and Thermotropic Layers. Energy Procedia 48, 1272–1281. doi:10.1016/j.egypro.2014.02.144

Goia, F., Perino, M., Haase, M., 2012a. A numerical model to evaluate the thermal behaviour of PCM glazing system configurations. Energy Build. 54, 141–153. doi:10.1016/j.enbuild.2012.07.036

Goia, F., Perino, M., Serra, V., 2014b. Experimental analysis of the energy performance of a full-scale PCM glazing prototype. Sol. Energy 100, 217–233. doi:10.1016/j.solener.2013.12.002

Goia, F., Perino, M., Serra, V., 2013. Improving thermal comfort conditions by means of PCM glazing systems. Energy Build. 60, 442–452. doi:10.1016/j.enbuild.2013.01.029

Goia, F., Zinzi, M., Carnielo, E., Serra, V., 2015. Spectral and angular solar properties of a PCM-filled double glazing unit. Energy Build. 87, 302–312. doi:10.1016/j.enbuild.2014.11.019

Goia, F., Zinzi, M., Carnielo, E., Serra, V., 2012b. Characterization of the optical properties of a PCM glazing system. Energy Procedia 30, 428–437. doi:10.1016/j.egypro.2012.11.051

Gowreesunker, B.L., Stankovic, S.B., Tassou, S.A., Kyriacou, P.A., 2013. Experimental and numerical investigations of the optical and thermal aspects of a PCM-glazed unit. Energy Build. 61, 239–249. doi:10.1016/j.enbuild.2013.02.032

Grynning, S., Goia, F., Rognvik, E., Time, B., 2013. Possibilities for characterization of a PCM window system using large scale measurements. Int. J. Sustain. Built Environ. 2, 56–64. doi:10.1016/j.ijsbe.2013.09.003

Grynning, S., Goia, F., Time, B., 2015. Dynamic Thermal Performance of a PCM Window System: Characterization Using Large Scale Measurements. Energy Procedia 78, 85–90. doi:10.1016/j.egypro.2015.11.119

Ismail, K.A.., Henríquez, J.., 2002. Parametric study on composite and PCM glass systems. Energy Convers. Manag. 43, 973–993. doi:10.1016/S0196-8904(01)00083-8

Ismail, K.A.R., Salinas, C.T., Henriquez, J.R., 2008. Comparison between PCM filled glass windows and absorbing gas filled windows. Energy Build. 40, 710–719. doi:10.1016/j.enbuild.2007.05.005

ISO 9050, 2003. Glass in building-determination of light transmittance, solar direct transmittance, total solar energy transmittance, ultraviolet transmittance and related glazing factors.

Kissok, J.K., Haberl, J.S., Claridge, D.E., 2003. Inverse Modeling Toolkit: Numerical Algorithms (RP-1050). Trans.-Am. Soc. Heat. Refrig. Air Cond. Eng. 109, 425–434.

Kissok, J.K., Xun, W., Sparks, R., Claridge, D.E., Haberl, J.S., 1994. EModel Version 1.4de. Copyr. Tex. AM Univ. Energy Systems Laboratory, Department of Mechanical Engineering, Texas A&M University, College Station, TX.

Li, D., Li, Z., Zheng, Y., Liu, C., Hussein, A.K., Liu, X., 2016a. Thermal performance of a PCM-filled double-glazing unit with different thermophysical parameters of PCM. Sol. Energy 133, 207–220. doi:10.1016/j.solener.2016.03.039

Li, D., Ma, T., Liu, C., Zheng, Y., Wang, Z., Liu, X., 2016b. Thermal performance of a PCM-filled double glazing unit with different optical properties of phase change material. Energy Build. 119, 143–152. doi:10.1016/j.enbuild.2016.03.036

Li, D., Zheng, Y., Li, Z., Qi, H., 2015. Optical properties of a liquid paraffin-filled double glazing unit. Energy Build. 108, 381–386. doi:10.1016/j.enbuild.2015.09.039

Li, S., Sun, G., Zou, K., Zhang, X., 2016. Experimental research on the dynamic thermal performance of a novel triple-pane building window filled with PCM. Sustain. Cities Soc. 27, 15–22. doi:10.1016/j.scs.2016.08.014
Liu, C., Zheng, Y., Li, D., Qi, H., Liu, X., 2016. A Model to Determine Thermal Performance of a Non-ventilated Double Glazing Unit with PCM and Experimental Validation. Procedia Eng. 157, 293–300. doi:10.1016/j.proeng.2016.08.369
Lyons P., Arasteh D., and H.C., 2000. Window performance for human thermal comfort, in: Proceeding of ASHRAE Winter Meeting, Dallas, TX, February 5-9. p. 92.
Seeboth, A., Ruhmann, R., Mühling, O., 2010. Thermotropic and Thermochromic Polymer Based Materials for Adaptive Solar Control. Materials 3, 5143–5168. doi:10.3390/ma3125143
Silva, T., Vicente, R., Rodrigues, F., 2016. Literature review on the use of phase change materials in glazing and shading solutions. Renew. Sustain. Energy Rev. 53, 515–535. doi:10.1016/j.rser.2015.07.201
Tukey, J.W., 1977. Exploratory data analysis, Addison-Wesley series in behavioral science. Addison-Wesley Pub. Co, Reading, Massachusetts.
Yao, J., Zhu, N., 2012. Evaluation of indoor thermal environmental, energy and daylighting performance of thermotropic windows. Build. Environ. 49, 283–290. doi:10.1016/j.buildenv.2011.06.004
Zhong, K., Li, S., Sun, G., Li, S., Zhang, X., 2015. Simulation study on dynamic heat transfer performance of PCM-filled glass window with different thermophysical parameters of phase change material. Energy Build. 106, 87–95. doi:10.1016/j.enbuild.2015.05.014

Acknowledgements

The research was started in the framework of “SMARTglass”, a project POR-FESR 2007-2013, funded by the Regione Piemonte and was part of the activities of the Cost Action TU1403 Adaptive Façades Network.

The authors would like to thank the Master degree students Alice Raffaelli, Federica Nigro, and Alice Pierleoni for their collaboration and help in the analysis of the experimental data.

Appendix 1

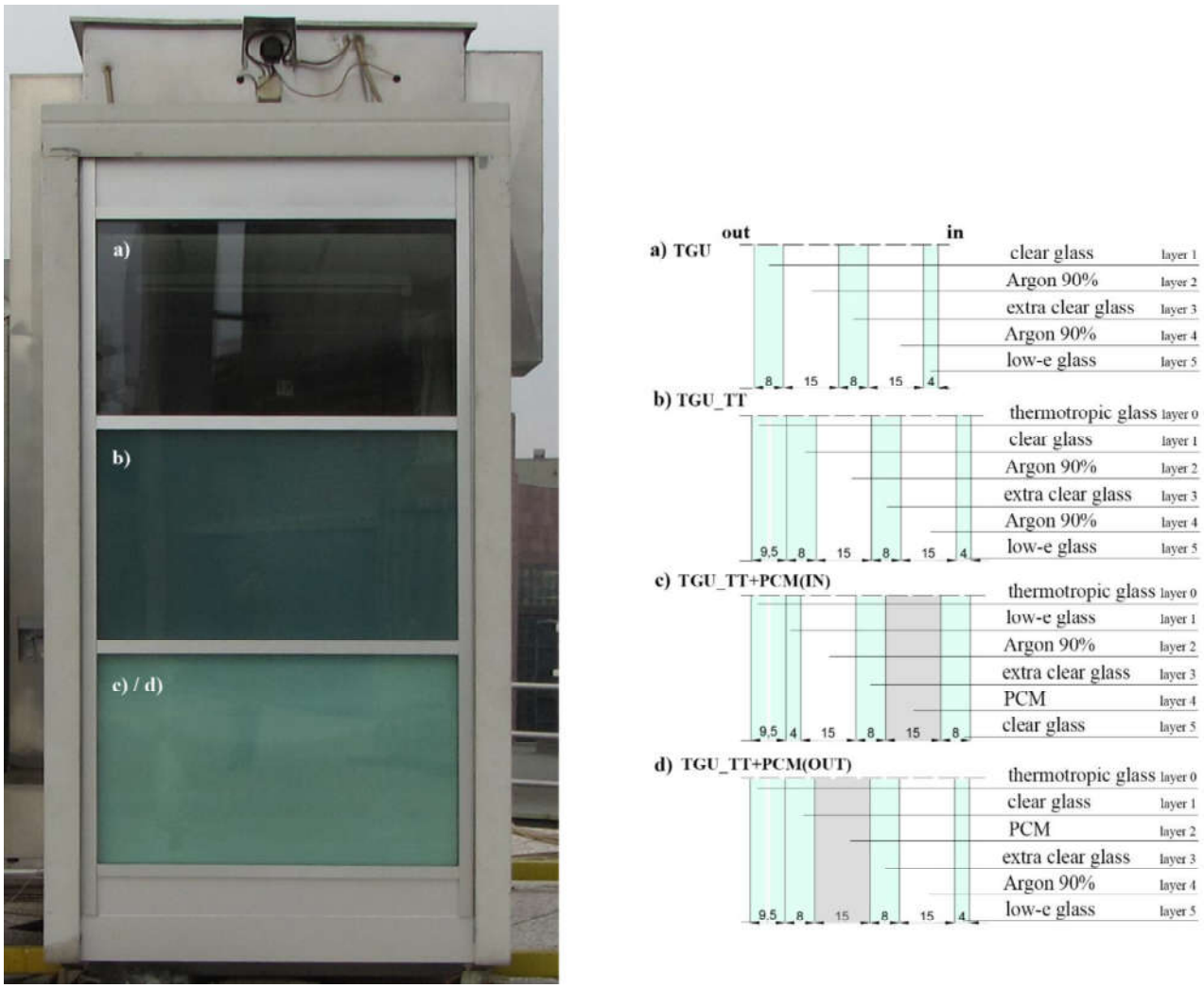

Fig.16 External view of the test cell (left) and scheme of the tested technologies (right) from Bianco et al. (2017).